LASER INTERFEROMETER GRAVITATIONAL WAVE OBSERVATORY
-LIGO-
CALIFORNIA INSTITUTE OF TECHNOLOGY
MASSACHUSETTS INSTITUTE OF TECHNOLOGY

Technical Note **LIGO-T080265- 00- Z** 10/06/08

A MATLAB model for the triple pendulum suspension system

Wan Wu

This is an internal working note
of the LIGO Project.

California Institute of Technology
LIGO Project - MS 18-34
Pasadena CA 91125
Phone (626) 395-2129
Fax (626) 304-9834
E-mail: info@ligo.caltech.edu

Massachusetts Institute of Technology
LIGO Project - MS NW17-161
Cambridge, MA 02139
Phone (617) 253-4824
Fax (617) 253-4824
E-mail: info@ligo.mit.edu

WWW: http://www.ligo.caltech.edu/

file /home/user/docs/T080265.pdf

1 Introduction

The modelling of the triple pendulum suspension system facilitates the analysis of the system's dynamic response to the external control forces or torques, providing a platform to evaluate the design modification. The matlab model described here is an independent approach to simulate the triple pendulum suspension installed in the JIF lab at the University of Glasgow. The analysis for the triple pendulum suspension system in this technical note only considers the control for the pendulum, not including the supporting isolation stacks. The comparison between this model and the previous model built by Torrie, etc.[1] helps check the accuracy of the model in parameterizing the pendulum.

Similar to the triple pendulum suspension for GEO 600 [2], the top mass of the pendulum is suspended from two cantilever springs using two wires. Four cantilever springs are mounted below the T-shape top mass, with the intermediate mass hung by the wires attached to these cantilevers. Another four wires hang the lower mass below the intermediate mass.

The pendulum is hung parallel to a reaction pendulum (see Figure 1). External control forces and torques can be applied to test masses via Integrated Optical position Sensor/ElectroMagnetic drivers (OSEMs). An OSEM consists of a flag magnet attached to one of the test masses, which is free to move between a light-emitting diode (LED) and a photo diode which are mounted on reaction masses accordingly. Motions of the magnet change the light intensity incident on the photo diode. Variations of the photo current introduced, is used as the error signal for the feed back control loop. The control signal is fed back to the coil mounted on the reaction mass, which applies electromagnetic force to pull or push the magnet back to the balanced position. Only the local control scheme (feedback control forces and torques are applied only on the top mass location) has been implemented for the Glasgow suspension system. And location of the six magnets on the top test mass can be viewed in Figure 1. Parameters of the pendulum are specified in Figure 4.

1.1 Mechanical Analysis

The response of the pendulum to external control forces and torques is analyzed using Newton's second law. Equations for motions of three masses in six degrees of freedom (DOF) and the transfer functions which characterize the frequency response of the upper test mass to external control forces and torques are given. Motions of the pendulum are limited to a small scale in order to ensure a linear control. Thus the mechanical analysis is based on the first order approximation for displacements of the pendulum of all 6 DOF.

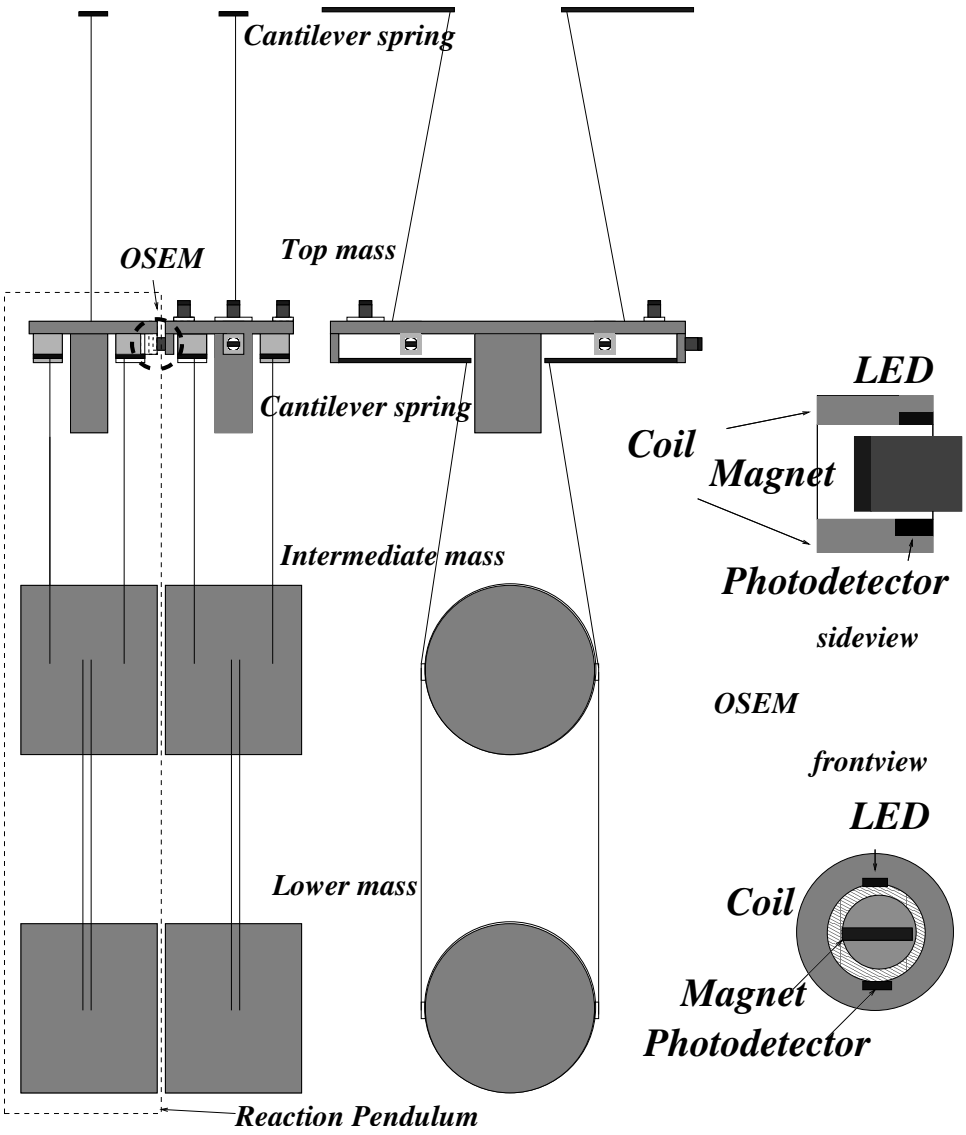

Figure 1: Schematic view of the triple pendulum.

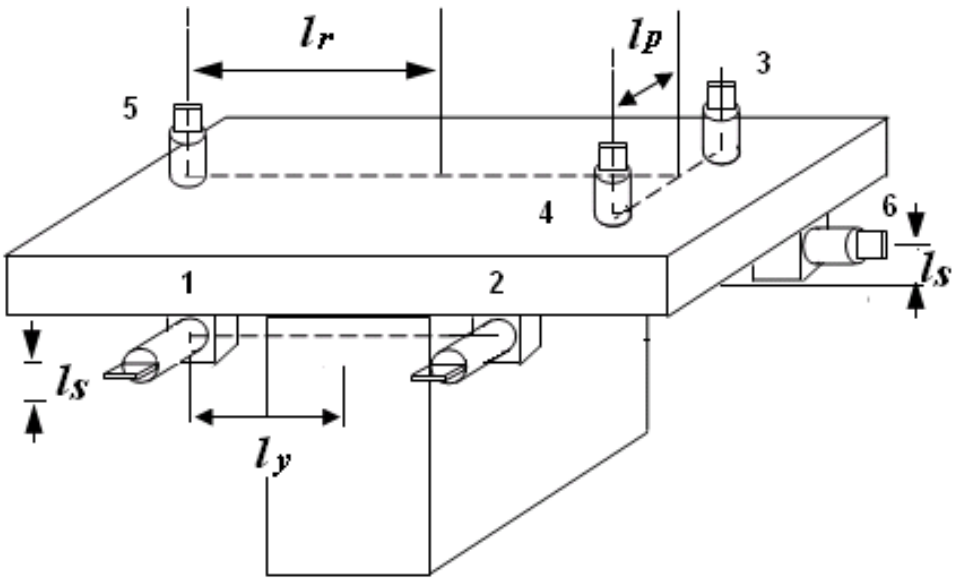

Figure 2: 'T-shape' top mass with six magnets attached. l_p - the half spacing of magnets (between 3 and 4) acting on pitch, l_y - the half spacing of magnets (between 1 and 2) acting on yaw, l_r - the half spacing of magnets (between the line along 3,4 and 5) acting on roll, l_s - the height of magnets 1, 2 and 6 above the center of mass.

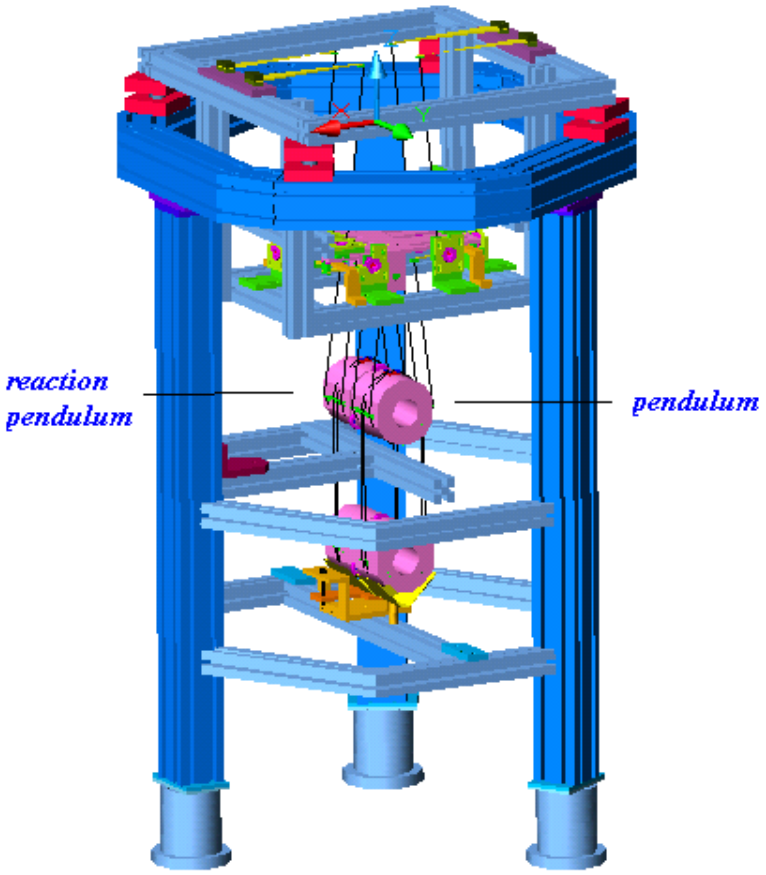

Figure 3: Three dimensional view of the triple pendulum suspension system.

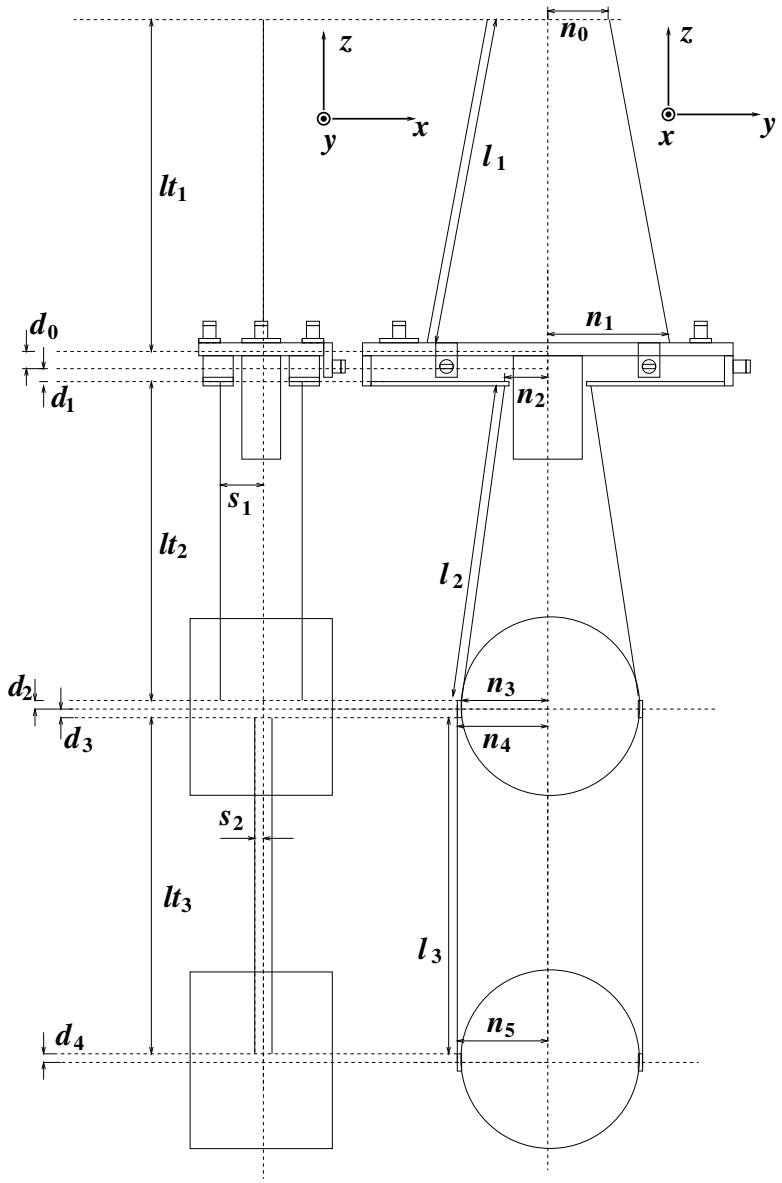

Figure 4: Parameters of a triple pendulum. s_1 and s_2 label half separations of suspension wires in the $\hat{x}$ direction. n_0, n_1, n_2, n_3, n_4, and n_5 label half separations of wires in the $\hat{y}$ direction at different suspension points. d_0, d_1, d_2, d_3, and d_4 label heights of the wire break-off points above or below the center of mass of different masses. Lengths of upper wires, intermediate wires and lower wires are represented as l_1, l_2, and l_3 respectively. And their projections on the vertical direction are l_{t1}, l_{t2}, and l_{t3}.

1.1.1 Vertical motion

Vertical motions of the pendulum remain uncoupled from the other five degrees of freedom motions. In a simplified case when a single pendulum is considered (see Figure 5), a vertical displacement Δz introduces a change in the length of the suspension wires. The length change Δl can be calculated to be

$$\Delta l = \Delta z \cos\Omega = \Delta z \frac{l_t}{l}. \tag{1}$$

Here Ω is the angle of the wires with respect to the vertical direction. Hence the vertical force applied on the mass due to the extension in the wire from the static equilibrium point is

$$F_h = k\Delta l \cos\Omega = k\Delta z \frac{{l_t}^2}{l^2}, \tag{2}$$

where k is the spring constant. Following this analysis, we can write down the equation for vertical motions of the lower test mass

$$m_3 \ddot{z}_3 = -4k_3 \left(z_3 - z_2\right) \frac{{l_{t3}}^2}{{l_3}^2}. \tag{3}$$

where z_3, z_2 represents vertical displacements of the lower test mass and the intermediate mass. Similarly, the equation for the intermediate mass is

$$m_2 \ddot{z}_2 = -4k_2 \left(z_2 - z_1\right) \frac{{l_{t2}}^2}{{l_2}^2} + 4k_3 \left(z_3 - z_2\right) \frac{{l_{t3}}^2}{{l_3}^2}. \tag{4}$$

Considering a control force F_v applied vertically on the upper mass via OSEMs, the equation for the upper mass is

$$m_1 \ddot{z}_1 = -2k_1 z_1 \frac{{l_{t1}}^2}{{l_1}^2} + 4k_2 \left(z_2 - z_1 \frac{{l_{t2}}^2}{{l_2}^2} + F_v\right). \tag{5}$$

To derive the transfer function, the above equations are rewritten in the Fourier domain, utilizing the transformation $z\left(t\right) = e^{i\omega t} z\left(\omega\right)$. These equations become

$$\begin{aligned}
-m_1 z_1 \omega^2 &= -2k_1 z_1 \tfrac{{l_{t1}}^2}{{l_1}^2} + 4k_2 \left(z_2 - z_1\right) \tfrac{{l_{t2}}^2}{{l_2}^2} + F_v, \\
-m_2 z_2 \omega^2 &= -2k_2 (z_2 - z_1) \frac{{l_{t2}}^2}{{l_2}^2} + 2k_3 \left(z_3 - z_2\right) \tfrac{{l_{t3}}^2}{{l_3}^2}, \\
-m_3 z_3 \omega^2 &= -2k_3 (z_3 - z_2) \frac{{l_{t3}}^2}{{l_3}^2}.
\end{aligned} \tag{6}$$

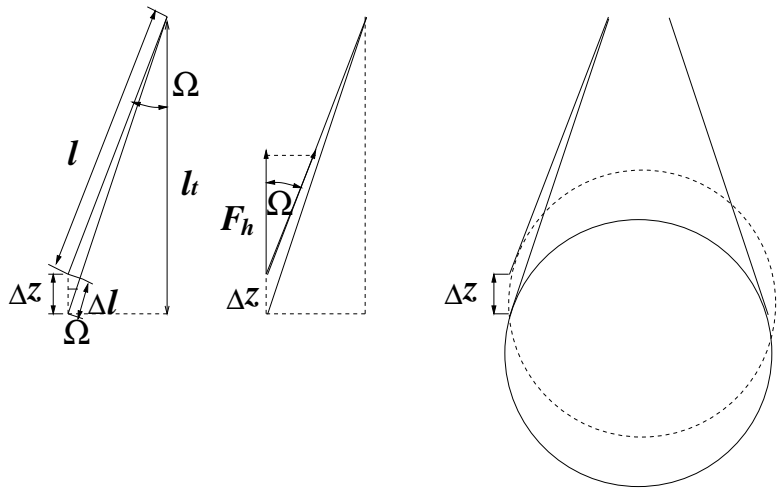

Figure 5: Vertical displacement of a single pendulum .

The relationship between the vertical control force and vertical motions of the upper mass can be described in the transfer function given below:

$$H_{zv}(\omega) = \frac{z_1}{F_v} = \cfrac{1}{m_1\omega^2 - 2k_1\frac{{l_{t1}}^2}{{l_1}^2} - 4k_2\frac{{l_{t2}}^2}{{l_2}^2} - \cfrac{16k_2^2}{m_2\omega^2 - 4k_2\frac{{l_{t2}}^2}{{l_2}^2} - 4k_3\frac{{l_{t3}}^2}{{l_3}^2} - \cfrac{16k_3^2\frac{{l_{t3}}^4}{{l_3}^4}}{m_3\omega^2 - 4k_3\frac{{l_{t3}}^2}{{l_3}^2}}}}. \tag{7}$$

Figure 6 is the Bode plot of the transfer function H_{zv}.

1.2 Longitudinal and Pitch Dynamics

The longitudinal motion in the $\hat{x}$-direction and the pitch motion are strongly coupled due to the fact that the break-off position of the wires are either above or below the line through the center of the mass. The tilt angle θ and the longitudinal displacement x will show up together as the variables in the linear differential equations that characterize the dynamics of the pendulum.
First, the dynamic equations of a single pendulum suspended from two wires of length l with a spring constant k are derived. Define s as the half separation between two suspension points and d as the height of the wire breaking off points above the center of mass. Figure 7 shows a single pendulum suspended by two wires. Consider the case when the mass is tilted by an angle θ from the horizontal line and displaced by x in the $\hat{x}$-direction. The wires are affected in opposite ways.

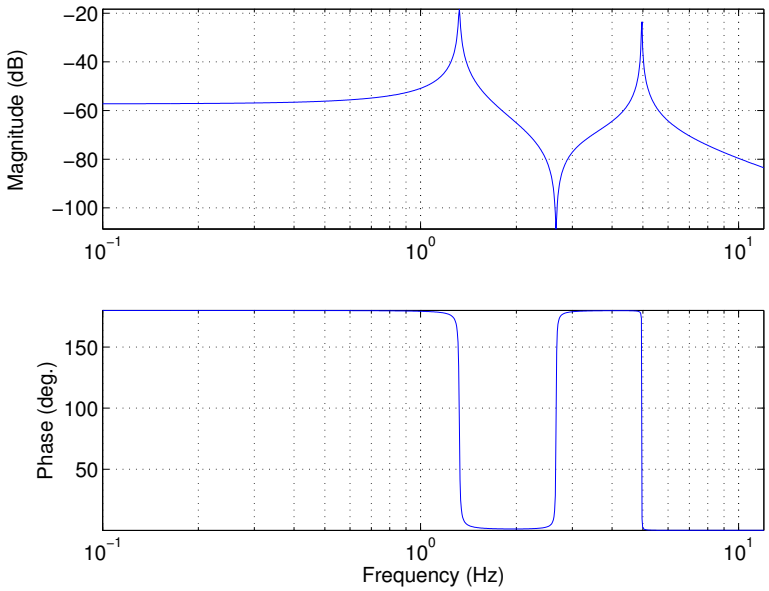

Figure 6: Bode plot of H_{zv}.

Wire 1 is contracted and wire 2 is stretched as can be seen in Figure 8. In Figure 8, the unfixed end of wire 1 moves from N to P'. MN is the displacement in the $\hat{x}$-direction.

$$|ON| = |NP| - |OP| = x - s, \tag{8}$$

$$|MO| = |RT| = \left|RO'\right| - \left|TO'\right| = s\cos\theta - d\sin\theta, \tag{9}$$

$$|MN| = |MO| + |ON| = s\cos\theta - d\sin\theta + x - s. \tag{10}$$

For a small angle θ and a small displacement x,

$$|MN| = x - d\theta. \tag{11}$$

$P'M$ is the displacement in the $\hat{y}$-direction.

$$|MR| = |OT| = s - s\cos\theta, \tag{12}$$

$$\left|P'M\right| = \left|P'R\right| - |MR|\,. \tag{13}$$

A small angle approximation gives,

$$\left|P'M\right| \approx s\theta. \tag{14}$$

So the length of wire 1 changes from the original length, l, to

$$l' = \sqrt{(l - s\theta)^2 + (x - d\theta)^2} \approx l - s\theta. \tag{15}$$

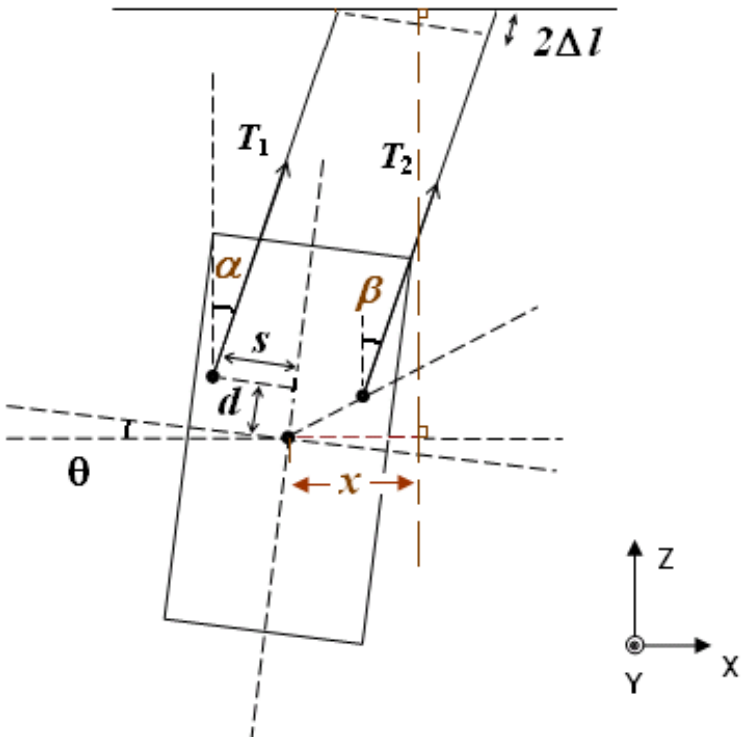

Figure 7: Side view of a single pendulum's longitudinal and pitch motion.

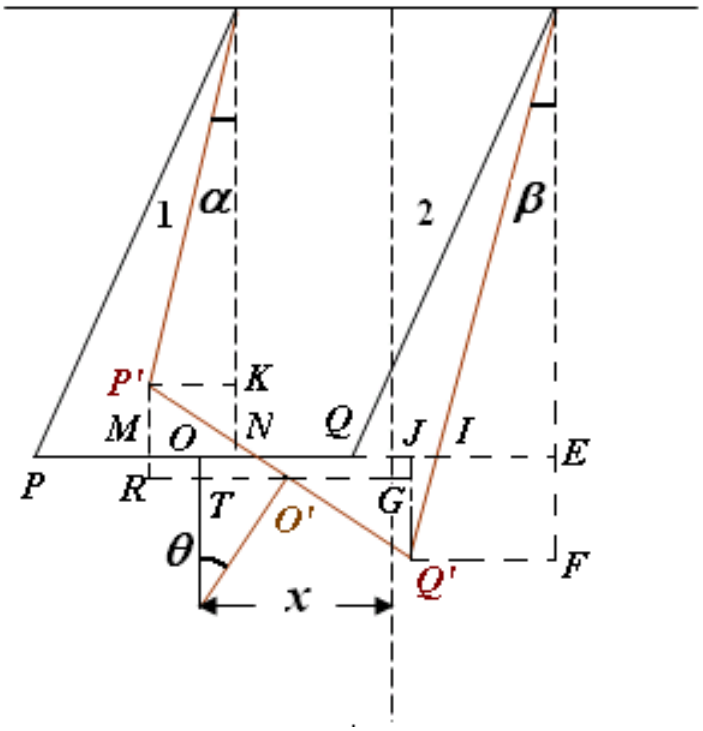

Figure 8: Longitudinal displacement introduced by the pitch motion.

Hence the change in the length of wire 1 is $\Delta l \approx s\theta$. We can also give

$$\sin\alpha \approx \frac{x - d\theta}{l}, \tag{16}$$

$$\cos\alpha \approx 1. \tag{17}$$

Similar geometric analysis shows us that wire 2 is stretched by Δl and

$$\sin\beta \approx \frac{x - d\theta}{l}, \tag{18}$$

$$\cos\beta \approx 1. \tag{19}$$

In an equilibrium state, the tension in each wire is

$$T_1 = T_2 = \frac{1}{2}mg. \tag{20}$$

Wire 1 is contracted such that in the first order approximation,

$$T_1 = \frac{1}{2}mg - k\Delta l. \tag{21}$$

And the tension in wire 2 becomes

$$T_2 = \frac{1}{2}mg + k\Delta l. \tag{22}$$

Hence the force on the mass along the $\hat{x}$-direction is

$$F = T_1 \sin\alpha + T_2 \sin\beta. \tag{23}$$

Substituting Equation 21 and 22 into Equation 23 gives

$$F = mg\frac{x - d\theta}{l}. \tag{24}$$

Finally, the equation for the longitudinal motion of a single pendulum suspended with two wires is

$$m\ddot{x} = -F \approx -mg\frac{x - d\theta}{l}. \tag{25}$$

The net torque which tilt the mass can be calculated as

$$Q = T_1\cos\alpha\,(s - d\theta) + T_1\sin\alpha(d + s\theta) - T_2\cos\beta\,(s + d\theta) + T_2\sin\beta(d - s\theta). \tag{26}$$

Substituting Equation 16, 17, 18, 19, 21 and 22 into 26 gives

$$Q \approx mg\frac{d}{l}x - \left(2ks^2 + mgd + mg\frac{d^2}{l}\right)\theta. \tag{27}$$

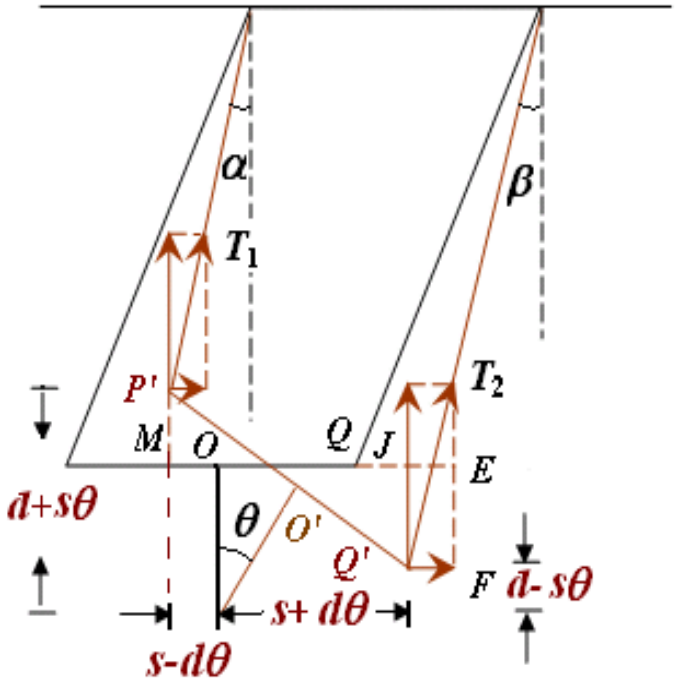

Figure 9: Components of restoring forces which act to tilt the mass.

Hence the equation of motion for pitch is

$$I\ddot{\theta} \approx \frac{mgd}{l}x - \left[2ks^2 + mg\left(d + \frac{d^2}{l}\right)\right]\theta. \tag{28}$$

The equations for the longitudinal/pitch motion of a triple pendulum can be derived based on the mechanical analysis of the single pendulum that is described above, i.e., the equations for each test mass can be given by simply modifying Equation 26 and 28. θ_i and x_i are used to define the tilt angle and the linear displacement of each mass of the triple pendulum (i = 1, 2, 3 - upper mass, intermediate mass and lower mass). The variables x and θ are replaced with the relative displacement of each mass with respect to the suspension points and the tilt angles between two adjacent masses. Hence for the lower mass, the equation for the longitudinal motion is

$$\ddot{x}_3 = -\frac{g}{l_{t3}}\left[(x_3 - x_2) - (d_4\theta_3 - d_3\theta_2)\right], \tag{29}$$

The equation for the pitch motion is

$$I_{3y}\ddot{\theta}_3 = \frac{m_3gd_4}{l_{t3}}(x_3 - x_2) - 4k_3s_2^2(\theta_3 - \theta_2) - m_3gd_4\left(\theta_3 + \frac{d_4\theta_3 - d_3\theta_2}{l_{t3}}\right). \tag{30}$$

The intermediate mass will be stretched by both the lower wires and the intermediate wires. The intermediate wires stretch the intermediate mass the same way that the lower wires do the lower mass while the lower wires affect the intermediate mass the opposite way according to Newton's third law. Now the tension along intermediate wires have to balance the gravity force introduced by both the intermediate mass and the lower mass. The dynamic equations for the intermediate mass are

$$m_2\ddot{x}_2 = -\frac{(m_2 + m_3)\,g}{l_{t2}}\left[(x_2 - x_1) - (d_2\theta_2 - d_1\theta_1)\right] + \frac{m_3g}{l_{t3}}\left[(x_3 - x_2) - (d_4\theta_3 - d_3\theta_2)\right], \tag{31}$$

$$I_{2y}\ddot{\theta}_2 = \frac{(m_2 + m_3)\,gd_2}{l_{t2}}(x_2 - x_1) - 4k_2s_1^2(\theta_2 - \theta_1) - (m_2 + m_3)\,gd_2\left(\theta_2 + \frac{d_2\theta_2 - d_1\theta_1}{l_{t2}}\right)$$
$$-\frac{m_3gd_3}{l_{t3}}(x_3 - x_2) + \left(4k_3 + \frac{m_3g}{l_{t3}}\right)s_2^2(\theta_3 - \theta_2) + m_3gd_3\left(\theta_3 + \frac{d_4\theta_3 - d_3\theta_2}{l_{t3}}\right). \tag{32}$$

There are only two wires above the upper mass. The tension in the wire is

$$T = \frac{1}{2}(m_1 + m_2 + m_3)g. \tag{33}$$

Both its vertical and horizontal components act to tilt the upper mass and the net torque is

$$Q = \frac{(m_1 + m_2 + m_3)\,gd_0}{l_{t1}}(x_1 - d_0\theta_1) - (m_1 + m_2 + m_3)\,gd_0\theta_1. \tag{34}$$

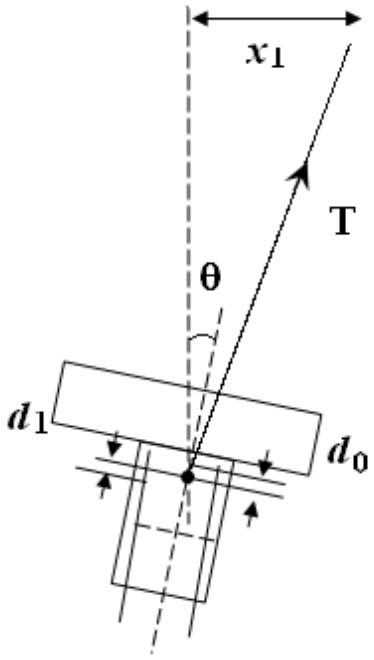

Figure 10: Side view of the top mass suspended with two wires.

The differential equations for the upper mass have the external control force and the control torque included. The force along the $\hat{x}$-direction F_l and the torque that controls the pitch motion, Q_p are applied via the OSEMs. In this case the equations become

$$I_{1y}\ddot{\theta}_1 = \frac{(m_1+m_2+m_3)\,gd_0}{l_{t1}}(x_1 - d_0\theta_1) - (m_1+m_2+m_3)\,gd_0\theta_1 - \frac{(m_2+m_3)\,gd_1}{l_{t2}}(x_2 - x_1) + 4k_2s_1^2(\theta_2-\theta_1) + (m_2+m_3)\,gd_1\left(\theta_2 + \frac{d_2\theta_2 - d_1\theta_1}{l_{t2}}\right) + Q_p, \tag{35}$$

$$m_1\ddot{x}_1 = -\frac{(m_1+m_2+m_3)\,g}{l_{t1}}(x_1 - d_0\theta_1) + \frac{(m_2+m_3)\,g}{l_{t2}}[(x_2-x_1) - (d_2\theta_2 - d_1\theta_1)] + F_l. \tag{36}$$

The Fourier transformation of Equation 29, 30, 31, 32, 35 and 36 gives:

$$x_2 - \left(1 - \omega^2\frac{l_{t3}}{g}\right)x_3 - d_3\theta_2 + d_4\theta_3 = 0, \tag{37}$$

$$-\frac{m_3gd_4}{l_{t3}}x_2 + \frac{m_3gd_4}{l_{t3}}x_3 + \left[4k_3s_2^2 + \frac{m_3g}{l_{t3}}d_4d_3\right]\theta_2 + \left[\omega^2 I_{3y} - 4k_3s_2^2 - m_3gd_4 - \frac{m_3g}{l_{t3}}\left(s_2^2+d_4^2\right)\right]\theta_3 = 0, \tag{38}$$

$$\frac{(m_2+m_3)\,g}{l_{t2}}x_1 + \left[m_2\omega^2 - \frac{(m_2+m_3)\,g}{l_{t2}} - \frac{m_3g}{l_{t3}}\right]x_2 + \frac{m_3g}{l_{t3}}x_3 - \frac{(m_2+m_3)\,g}{l_{t2}}d_1\theta_1 + \left[\frac{m_3g}{l_{t3}}d_3 + \frac{(m_2+m_3)\,g}{l_{t2}}d_2\right]\theta_2 - \frac{m_3g}{l_{t3}}d_4\theta_3 = 0, \tag{39}$$

$$-\frac{(m_2+m_3)\,gd_2}{l_{t2}}x_1 + \left[\frac{(m_2+m_3)\,gd_2}{l_{t2}} + \frac{m_3gd_3}{l_{t3}}\right]x_2 - \frac{m_3gd_3}{l_{t3}}x_3 + \left[4k_2s_1^2 + \frac{(m_2+m_3)\,g}{l_{t2}}d_1d_2\right]\theta_1 + \left[\omega^2 I_{2y} - 4k_2s_1^2 - \frac{(m_2+m_3)\,g}{l_{t2}}d_2^2 - (m_2+m_3)\,gd_2 - 4k_3s_2^2 - \frac{m_3g}{l_{t3}}d_3^2\right]\theta_2 + \left[4k_3s_2^2 + \frac{m_3g}{l_{t3}}d_3d_4 + m_3gd_3\right]\theta_3 = 0\ , \tag{40}$$

$$\left[m_1\omega^2 - \frac{(m_2+m_3)\,g}{l_{t2}} - \frac{(m_1+m_2+m_3)\,g}{l_{t1}}\right]x_1 + \frac{(m_2+m_3)\,g}{l_{t2}}x_2 + \left[\frac{(m_1+m_2+m_3)\,g}{l_{t1}}d_0 + \frac{(m_2+m_3)\,g}{l_{t2}}d_1\right]\theta_1 - \frac{(m_2+m_3)\,g}{l_{t2}}d_2\theta_2 = F_l, \tag{41}$$

and

$$\left[\frac{(m_1+m_2+m_3)\,gd_0}{l_{t1}}+\frac{(m_2+m_3)\,gd_1}{l_{t2}}\right]x_1-\frac{(m_2+m_3)\,gd_1}{l_{t2}}x_2+\left[\omega^2 I_{1y}-4k_2s_1^2-\frac{gd_0^2}{l_{t1}}\right.$$
$$\left.(m_1+m_2+m_3)-(m_1+m_2+m_3)\,gd_0-\frac{(m_2+m_3)\,g}{l_{t2}}d_1^2\right]\theta_1+\Big[(m_2+m_3)\,gd_1$$
$$\left.+4k_2s_1^2+\frac{(m_2+m_3)\,g}{l_{t2}}d_1d_2\right]\theta_2=Q_p. \tag{42}$$

These equations can be written in a matrix form:

$$\begin{pmatrix}\Gamma_{11}&\Gamma_{12}&0&\Gamma_{14}&\Gamma_{15}&0\\ \Gamma_{21}&\Gamma_{22}&\Gamma_{23}&\Gamma_{24}&\Gamma_{25}&\Gamma_{26}\\ 0&\Gamma_{32}&\Gamma_{33}&0&\Gamma_{35}&\Gamma_{36}\\ \Gamma_{41}&\Gamma_{42}&0&\Gamma_{44}&\Gamma_{45}&0\\ \Gamma_{51}&\Gamma_{52}&\Gamma_{53}&\Gamma_{54}&\Gamma_{55}&\Gamma_{56}\\ 0&\Gamma_{62}&\Gamma_{63}&0&\Gamma_{65}&\Gamma_{66}\end{pmatrix}\begin{pmatrix}x_1\\x_2\\x_3\\\theta_1\\\theta_2\\\theta_3\end{pmatrix}=\begin{pmatrix}F_l\\0\\0\\Q_p\\0\\0\end{pmatrix}. \tag{43}$$

Here,

$$\Gamma_{11}=m_1\omega^2-\frac{(m_2+m_3)\,g}{l_{t2}}-\frac{(m_1+m_2+m_3)\,g}{l_{t1}}, \tag{44}$$

$$\Gamma_{12}=\frac{(m_2+m_3)\,g}{l_{t2}}, \tag{45}$$

$$\Gamma_{14}=\frac{(m_1+m_2+m_3)\,g}{l_{t1}}d_0+\frac{(m_2+m_3)\,g}{l_{t2}}d_1, \tag{46}$$

$$\Gamma_{15}=-\frac{(m_2+m_3)\,g}{l_{t2}}d_2, \tag{47}$$

$$\Gamma_{21}=\frac{(m_2+m_3)\,g}{l_{t2}}, \tag{48}$$

$$\Gamma_{22}=m_2\omega^2-\frac{(m_2+m_3)\,g}{l_{t2}}-\frac{m_3g}{l_{t3}}, \tag{49}$$

$$\Gamma_{23}=\frac{m_3g}{l_{t3}}, \tag{50}$$

$$\Gamma_{24}=-\frac{(m_2+m_3)\,g}{l_{t2}}d_1, \tag{51}$$

$$\Gamma_{25}=\frac{(m_2+m_3)\,g}{l_{t2}}d_2+\frac{m_3g}{l_{t3}}d_3, \tag{52}$$

$$\Gamma_{26}=-\frac{m_3g}{l_{t3}}d_4, \tag{53}$$

$$\Gamma_{32}=1, \tag{54}$$

$$\Gamma_{33} = \omega^2 \frac{l_{t3}}{g} - 1, \tag{55}$$

$$\Gamma_{35} = -d_3, \tag{56}$$

$$\Gamma_{36} = d_4, \tag{57}$$

$$\Gamma_{41} = \frac{(m_1 + m_2 + m_3)\, g d_0}{l_{t1}} + \frac{(m_2 + m_3)\, g d_1}{l_{t2}}, \tag{58}$$

$$\Gamma_{42} = -\frac{(m_2 + m_3)\, g d_1,}{l_{t2}} \tag{59}$$

$$\Gamma_{44} = \omega^2 I_{1y} - 4k_2 s_1^2 - \frac{(m_1 + m_2 + m_3)\, g d_0}{l_{t1}} d_0 - (m_1 + m_2 + m_3)\, g d_0 - \frac{(m_2 + m_3)\, g}{l_{t2}} d_1^2, \tag{60}$$

$$\Gamma_{45} = 4k_2 s_1^2 + (m_2 + m_3)\, g d_1 + \frac{(m_2 + m_3)\, g}{l_{t2}} d_1 d_2, \tag{61}$$

$$\Gamma_{51} = -\frac{(m_2 + m_3)\, g d_2}{l_{t2}}, \tag{62}$$

$$\Gamma_{52} = \frac{(m_2 + m_3)\, g d_2}{l_{t2}} + \frac{m_3 g d_3}{l_{t3}}, \tag{63}$$

$$\Gamma_{53} = -\frac{m_3 g d_3}{l_{t3}}, \tag{64}$$

$$\Gamma_{54} = 4k_2 s_1^2 + \frac{(m_2 + m_3)\, g}{l_{t2}} d_1 d_2, \tag{65}$$

$$\Gamma_{55} = \omega^2 I_{2y} - 4k_2 s_1^2 - \frac{(m_2 + m_3)\, g}{l_{t2}} d_2^2 - (m_2 + m_3)\, g d_2 - 4k_3 s_2^2 - \frac{m_3 g}{l_{t3}} d_3^2, \tag{66}$$

$$\Gamma_{56} = 4k_3 s_2^2 + \frac{m_3 g}{l_{t3}} d_3 d_4 + m_3 g d_3, \tag{67}$$

$$\Gamma_{62} = -\frac{m_3 g d_4}{l_{t3}}, \tag{68}$$

$$\Gamma_{63} = \frac{m_3 g d_4}{l_{t3}}, \tag{69}$$

$$\Gamma_{65} = 4k_3 s_2^2 + \frac{m_3 g}{l_{t3}} d_4 d_3, \tag{70}$$

and

$$\Gamma_{66} = \omega^2 I_{3y} - 4k_3 s_2^2 - m_3 g d_4 - \frac{m_3 g}{l_{t3}} d_4^2. \tag{71}$$

Thus the response of the triple pendulum to the external force applied in the longitudinal direction and the torque that tilts the top mass can be calculated as

$$\begin{pmatrix} x_1 \\ x_2 \\ x_3 \\ \theta_1 \\ \theta_2 \\ \theta_3 \end{pmatrix} = T \begin{pmatrix} F_l \\ 0 \\ 0 \\ Q_p \\ 0 \\ 0 \end{pmatrix}. \tag{72}$$

where $T = \Gamma^{-1}$. The response of the top mass to F_l and Q_p can be analytically calculated as

$$H_{xl} = \frac{x_1}{F_l} = T_{11}, \tag{73}$$

$$H_{xp} = \frac{x_1}{Q_p} = T_{14}, \tag{74}$$

$$H_{\theta l} = \frac{\theta_1}{F_l} = T_{41}, \tag{75}$$

and

$$H_{\theta p} = \frac{\theta_1}{Q_p} = T_{44}. \tag{76}$$

These transfer functions are plotted in Figure 11, Figure 12, Figure 13, and Figure 14 respectively.

1.3 Yaw Motion

First, we consider the case of a mass suspended by four wires of length l, which are all at the same angle Ω with respect to the vertical direction as is shown in Figure 15. The tension T in one wire can be projected along two directions. The vertical component T_v balances the gravity force while the horizontal component T_h along the direction $\overrightarrow{BD}$ is balanced by the horizontal force introduced from another wire. However, when the mass rotates through an angle ϕ, the net torque by the horizontal components of the tension force of four wires will not keep the mass in a balanced state any longer. In Figure 16 we can clearly see that it is the force F that acts to rotate the mass. F is the projection of T_h in the direction perpendicular to the line connecting the suspension point and the center of mass,

$$F = T_h \cos\gamma \tag{77}$$

where

$$T_h = T_v \tan\Omega_t = \frac{1}{4} mg \frac{|BD|}{|CD|} \tag{78}$$

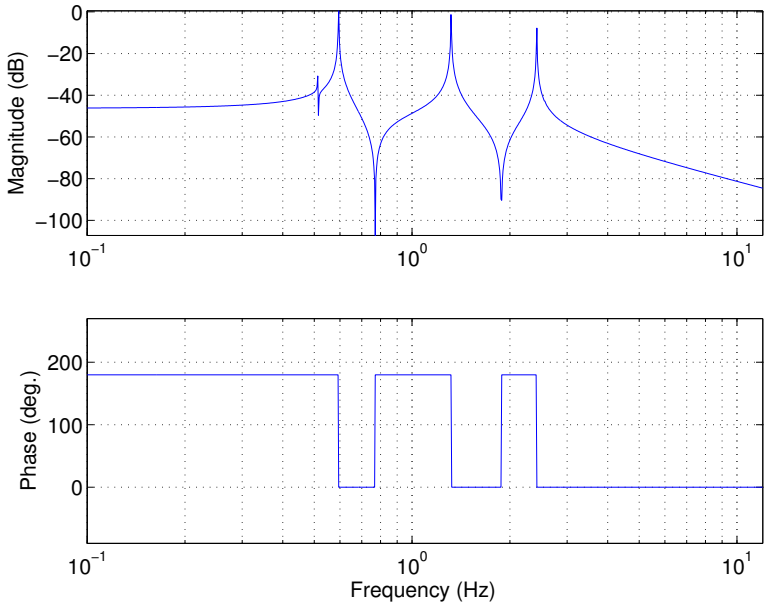

Figure 11: Bode plot of H_{xl}.

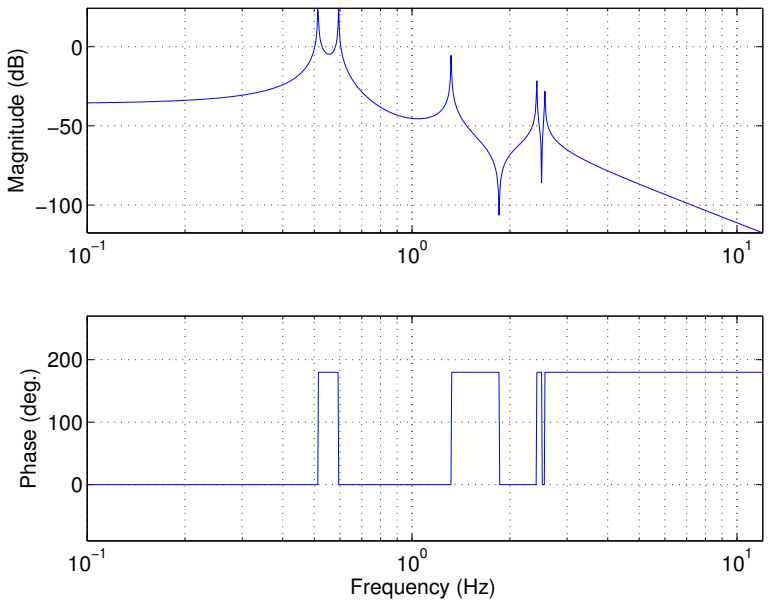

Figure 12: Bode plot of H_{xp}.

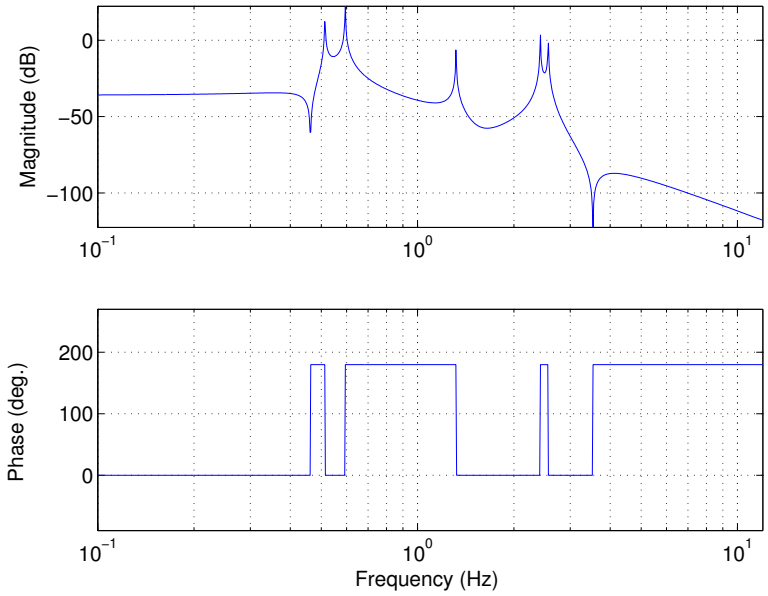

Figure 13: Bode plot of $H_{\theta l}$.

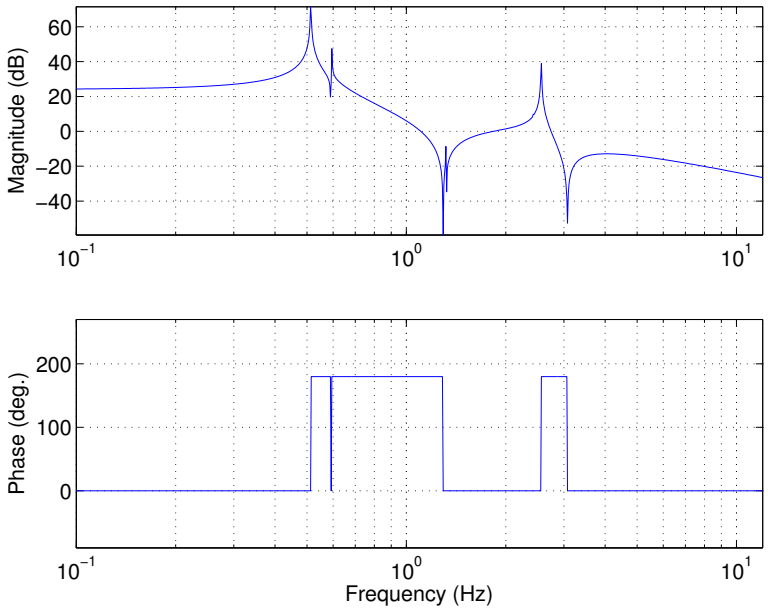

Figure 14: Bode plot of $H_{\theta p}$.

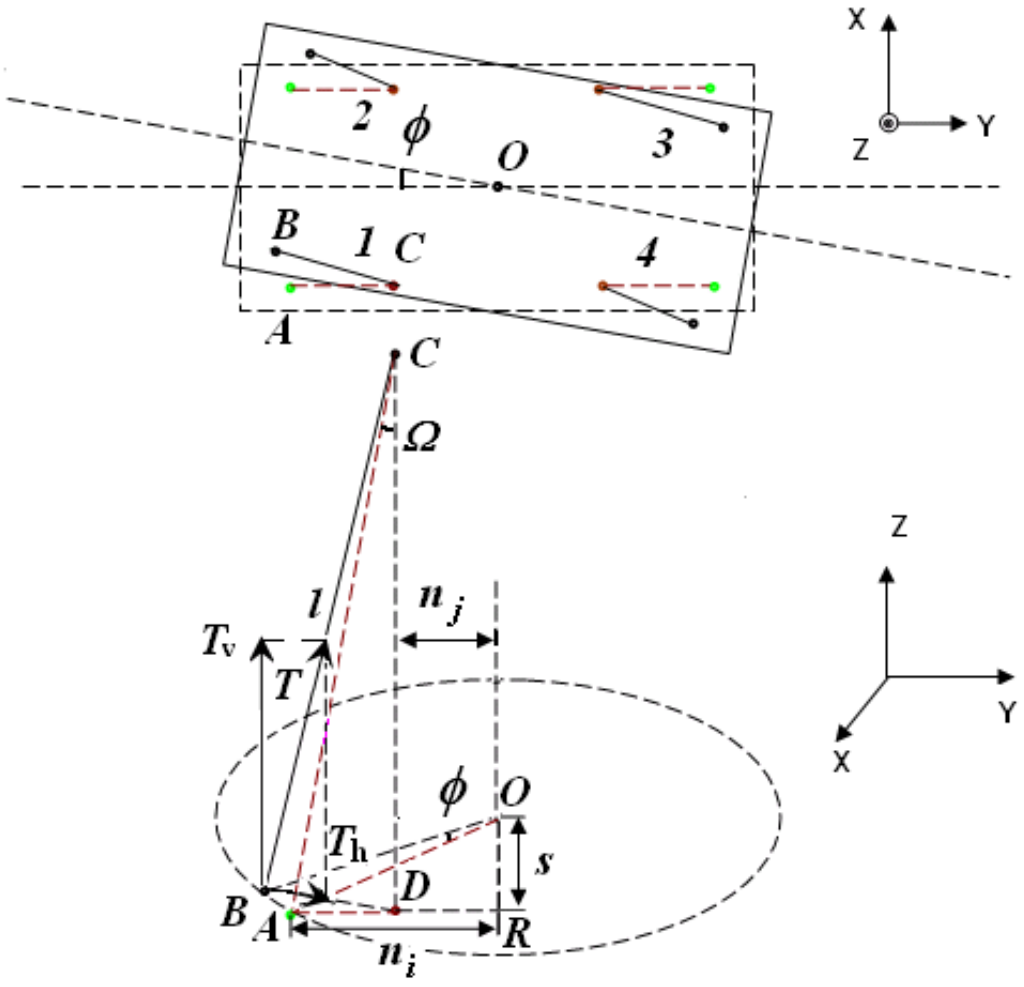

Figure 15: Yaw displacement of a single pendulum. The upper part is the view from above. And the low part is the geometric plot of the effect on one wire when the mass is rotated through an angle ϕ.

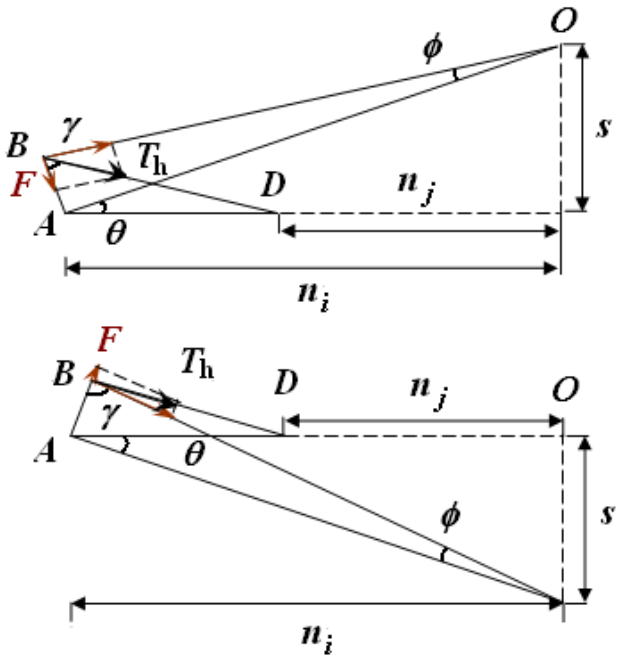

Figure 16: Projection of the tension force T (see Figure 15) onto $\hat{x}$-$\hat{y}$ plane which produces the restoring torque. The upper plot and the lower plot are associated with two different effects on wires when the mass rotates.

and

$$\cos\gamma = \frac{|AB|^2 + |BD|^2 - |AD|^2}{2\,|AB|\,|BD|}. \tag{79}$$

$|AB|$ and $|AD|$ are determined by the parameters given by the dimensions of the mass:

$$|AB| = \sqrt{\left(s^2 + n_i^2\right)}\phi, \tag{80}$$

$$|AD| = n_i - n_j. \tag{81}$$

$|BD|$ is calculated from $|AB|$ and $|AD|$,

$$|BD| = \sqrt{|AB|^2 + |AD|^2 - 2\,|AB|\,|AD|\cos\angle BAD}. \tag{82}$$

Here $\angle BAD$ can be $90^\circ + \theta$ or $90^\circ - \theta$, depending on whether a wire stretches or contracts when the mass rotates. In Figure 15, wires 1 and 3 stretch while wires 2 and 4 contract when the mass rotates in a clockwise direction. The stretch and the contraction change $|BD|$ such that

$$|BD_\pm| = \sqrt{\left(s^2 + n_i^2\right)\phi^2 + \left(n_i - n_j\right)^2 \pm 2\sqrt{s^2 + n_i^2}\left(n_i - n_j\right)\sin\theta\phi} \approx n_i - n_j \pm s\phi \tag{83}$$

Therefore, we can write T_h and $\cos\gamma$ as

$$\begin{aligned}
\cos\gamma_\pm &= \frac{\left(s^2 + n_i^2\right)\phi^2 + \left(s^2 + n_i^2\right)\phi^2 + \left(n_i - n_j\right)^2 \pm 2\sqrt{s^2 + n_i^2}\left(n_i - n_j\right)\sin\theta\phi - \left(n_i - n_j\right)^2}{2\sqrt{s^2 + n_i^2}\phi\left(n_i - n_j \pm \sqrt{s^2 + n_i^2}\sin\theta\phi\right)} \\
&= \frac{\sqrt{s^2 + n_i^2}\phi \pm \left(n_i - n_j\right)\sin\theta}{\left(n_i - n_j\right)\left(1 \pm \dfrac{\sqrt{s^2 + n_i^2}\sin\theta\phi}{n_i - n_j}\right)} \approx \left(\frac{\sqrt{s^2 + n_i^2}\phi}{n_i - n_j} \pm \sin\theta\right)\left(1 \mp \frac{\sqrt{s^2 + n_i^2}\sin\theta\phi}{n_i - n_j}\right) \\
&\approx \frac{\sqrt{s^2 + n_i^2}\cos^2\theta}{n_i - n_j}\phi \pm \sin\theta = \frac{n_i\cos\theta}{n_i - n_j}\phi \pm \sin\theta,
\end{aligned} \tag{84}$$

$$T_{h\pm} = \frac{1}{4}mg\frac{n_i - n_j \pm s\phi}{\sqrt{l^2 - \left(n_i - n_j\right)^2}}. \tag{85}$$

Now the total torque from four wires is

$$\begin{aligned}
Q &= 2T_{h+}\cos\gamma_+\sqrt{s^2 + n_i^2} + 2T_{h-}\cos\gamma_-\sqrt{s^2 + n_i^2} \approx \frac{1}{2}mg\frac{n_i - n_j + s\phi}{\sqrt{l^2 - \left(n_i - n_j\right)^2}}\left(\frac{n_i^2}{n_i - n_j}\phi + s\right) \\
&+ \frac{1}{2}mg\frac{n_i - n_j - s\phi}{\sqrt{l^2 - \left(n_i - n_j\right)^2}}\left(\frac{n_i^2}{n_i - n_j}\phi - s\right) = \frac{mg\left(n_i^2 + s^2\right)}{\sqrt{l^2 - \left(n_i - n_j\right)^2}}\phi.
\end{aligned} \tag{86}$$

Hence the equation of motion for a four wire suspension is

$$I\ddot{\phi} = -\frac{mg\left(n_i^2 + s^2\right)}{\sqrt{l^2 - \left(n_i - n_j\right)^2}}\phi. \tag{87}$$

Similar to what is outlined in the longitudinal and pith case, the differential equation can be extended to describe the yaw motion of a triple pendulum in terms of the rotation angle of each mass with respect to the suspension points of each stage. The tension in the wires of each stage is proportional to the total weight of the masses below the wires. The equations of the yaw motion for the lower mass and the intermediate mass are therefore

$$I_{3z}\ddot{\phi}_3 = -\frac{m_3 g\left(n_5^2 + s_2^2\right)}{\sqrt{l^2 - \left(n_5 - n_4\right)^2}}\left(\phi_3 - \phi_2\right), \tag{88}$$

and

$$I_{2z}\ddot{\phi}_2 = -\frac{\left(m_2 + m_3\right) g\left(n_3^2 + s_1^2\right)}{l_{t2}}\left(\phi_2 - \phi_1\right)\phi_2 + \frac{m_3 g\left(n_4^2 + s_2^2\right)}{l_{t3}}\left(\phi_3 - \phi_2\right). \tag{89}$$

The line determined by the two upper suspension points on the top mass passes through the center of mass. So the horizontal components of tensions in two upper suspension wire can be written in a relatively simpler form

$$T_h = \frac{1}{2}\left(m_1 + m_2 + m_3\right) g\frac{n_1 - n_0}{l_{t1}}. \tag{90}$$

This produces a torque on the top mass when the mass is rotated by a small angle ϕ,

$$Q = \left(m_1 + m_2 + m_3\right) g\frac{{n_1}^2}{l_{t1}^2}\phi. \tag{91}$$

Therefore the differential equation which describes the yaw motion of the upper mass becomes

$$I_{1z}\ddot{\phi}_1 = -\frac{\left(m_1 + m_2 + m_3\right) g n_1^2}{l_{t1}}\phi_1 + \frac{\left(m_2 + m_3\right) g\left(n_3^2 + s_1^2\right)}{l_{t2}}\left(\phi_2 - \phi_1\right) + Q_y, \tag{92}$$

where Q_y is the external feedback torque used to stabilize the yaw motion of the top mass. The Fourier transform of Equation 88, 89 and 92 are listed below,

$$\omega^2 I_{3z}\phi_3 = \frac{m_3 g\left(n_5^2 + s_2^2\right)}{l_{t3}}\left(\phi_3 - \phi_2\right), \tag{93}$$

$$\omega^2 I_{2z}\phi_2 = \frac{\left(m_2 + m_3\right) g\left(n_3^2 + s_1^2\right)}{l_{t2}}\left(\phi_2 - \phi_1\right) - \frac{m_3 g\left(n_4^2 + s_2^2\right)}{l_{t3}}\left(\phi_3 - \phi_2\right), \tag{94}$$

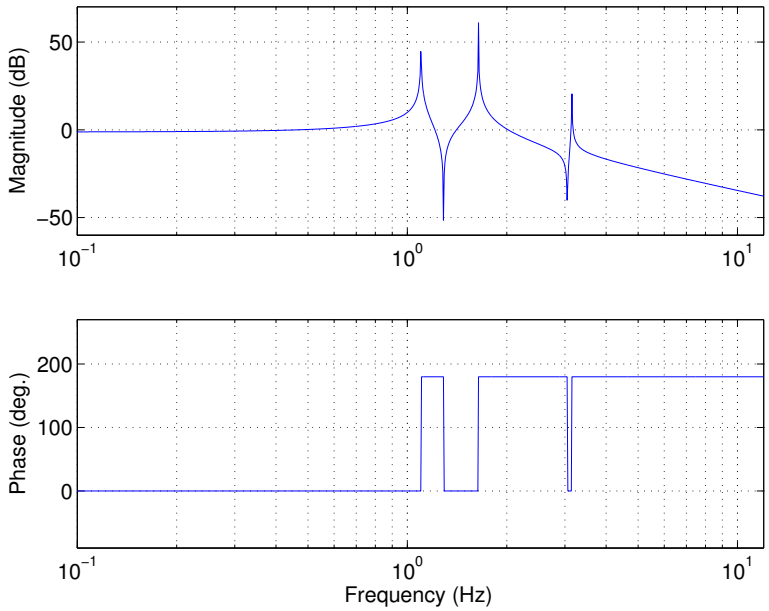

Figure 17: Bode plot of $H_{\phi y}$.

$$\omega^2 I_{1z}\phi_1 = \frac{(m_1+m_2+m_3)\,gn_1^2}{l_{t1}}\phi_1 - \frac{(m_2+m_3)\,g\left(n_2^2+s_1^2\right)}{l_{t2}}\left(\phi_2-\phi_1\right) - Q_y. \quad (95)$$

From Equation 1.3, 94 and 95, the transfer function that relates the external torque Q_y to the induced rotation of the top mass ϕ_1 is derived as

$$H_{\phi y} = \frac{\phi_1}{Q_y} = \left\{ \frac{(m_1+m_2+m_3)\,gn_1^2}{l_{t1}} - \omega^2 I_{1z} + \frac{(m_2+m_3)\,g\left(n_2^2+s_1^2\right)}{l_{t2}} \right.$$
$$\left. \left(\frac{\dfrac{m_3 g\left(n_4^2+s_2^2\right)}{l_{t3}}\left(1-\dfrac{m_3 g\left(n_5^2+s_2^2\right)}{m_3 g\left(n_5^2+s_2^2\right)-\omega^2 l_{t3} I_{3z}}\right) - \omega^2 I_{2z}}{\dfrac{(m_2+m_3)\,g\left(n_3^2+s_1^2\right)}{l_{t2}} + \dfrac{m_3 g\left(n_4^2+s_2^2\right)}{l_{t3}}\left(1-\dfrac{m_3 g\left(n_5^2+s_2^2\right)}{m_3 g\left(n_5^2+s_2^2\right)-\omega^2 l_{t3} I_{3z}}\right) - \omega^2 I_{2z}} \right) \right\}. \quad (96)$$

The transfer function $H_{\phi y}$ is plotted in Figure 17.

1.4 Sideways and Roll Motion

The coupling between the sideways and the roll motion is similar to the coupling between the longitudinal and the pitch motion. However, sideways and roll coupling is more complicated. The wires that are used to suspend the masses are angled in the $\hat{y}$-direction. The sideways motion of the mass will create a torque that can

excite the roll motion while the longitudinal displacement does not tilt the mass. The details will be discussed below.

Consider a single pendulum suspended with two wires as is plotted in Figure 18. The two wires have the same length l in the equilibrium state. And the tensions in both wires are,

$$T_1 = T_2 = \frac{1}{2} mg \frac{l}{l_t} \tag{97}$$

After the mass is displaced by a small distance y in the $\hat{y}$-direction, the center of mass moves from O to P. This is followed by a mass rolling by a small angle φ. The suspension points now move from G and J to E and F. Thus the new lengths of the two wires can be derived. From Figure 18 and Figure 19,

$$|AE|^2 = |KH|^2 + l_t^2, \tag{98}$$

$$\begin{aligned} |AE| &= \sqrt{(n_j - n_i + y - d\varphi)^2 + (l_t - n_j\varphi)^2} \approx \sqrt{(n_j - n_i)^2 + 2(n_j - n_i)(y - d\varphi) + l_t^2 - 2n_j l_t \varphi} \\ &= \sqrt{l^2 + 2(n_j - n_i)\, y - 2(n_j l_t + n_j d - n_i d)\, \varphi} \approx l + \frac{n_j - n_i}{l} y - \frac{n_j l_t + n_j d - n_i d}{l} \varphi. \end{aligned} \tag{99}$$

Hence wire 1 is stretched by

$$\Delta l = \frac{n_j - n_i}{l} y - \frac{n_j l_t + n_j d - n_i d}{l} \varphi. \tag{100}$$

And for wire 2,

$$|BF|^2 = |LI|^2 + |l_t + |FL||^2, \tag{101}$$

$$\begin{aligned} |BF| &= \sqrt{(y - (n_j - n_i) - d\varphi)^2 + (l_t + n_j\varphi)^2} \approx \sqrt{(n_j - n_i)^2 - 2(n_j - n_i)(y - d\varphi) + l_t^2 + 2n_j l_t \varphi} \\ &= \sqrt{l^2 - 2(n_j - n_i)\, y + 2(n_j l_t + n_j d - n_i d)\, \varphi} \approx l - \frac{n_j - n_i}{l} y + \frac{n_j l_t + n_j d - n_i d}{l} \varphi. \end{aligned} \tag{102}$$

Wire 2 is then contracted by Δl. Now the tensions in wire 1 and wire 2 become

$$T_1 = \frac{1}{2} mg \frac{l}{l_t} + k\Delta l, \tag{103}$$

$$T_2 = \frac{1}{2} mg \frac{l}{l_t} - k\Delta l. \tag{104}$$

The angle of wire 1 with respect to the vertical direction Ω_1 satisfies

$$\sin\Omega_1 = \frac{n_j - n_i}{l} + \left[\frac{1}{l} - \frac{(n_j - n_i)^2}{l^3}\right] y - \left[\frac{d}{l} - \frac{(n_j - n_i)(n_j l_t + n_j d - n_i d)}{l^3}\right] \varphi, \tag{105}$$

and

$$\cos\Omega_1 = \frac{l_t}{l} - \frac{(n_j - n_i)\, l_t}{l^3} y - \left[\frac{n_j}{l} - \frac{l_t (n_j l_t + n_j d - n_i d)}{l^3}\right] \varphi. \tag{106}$$

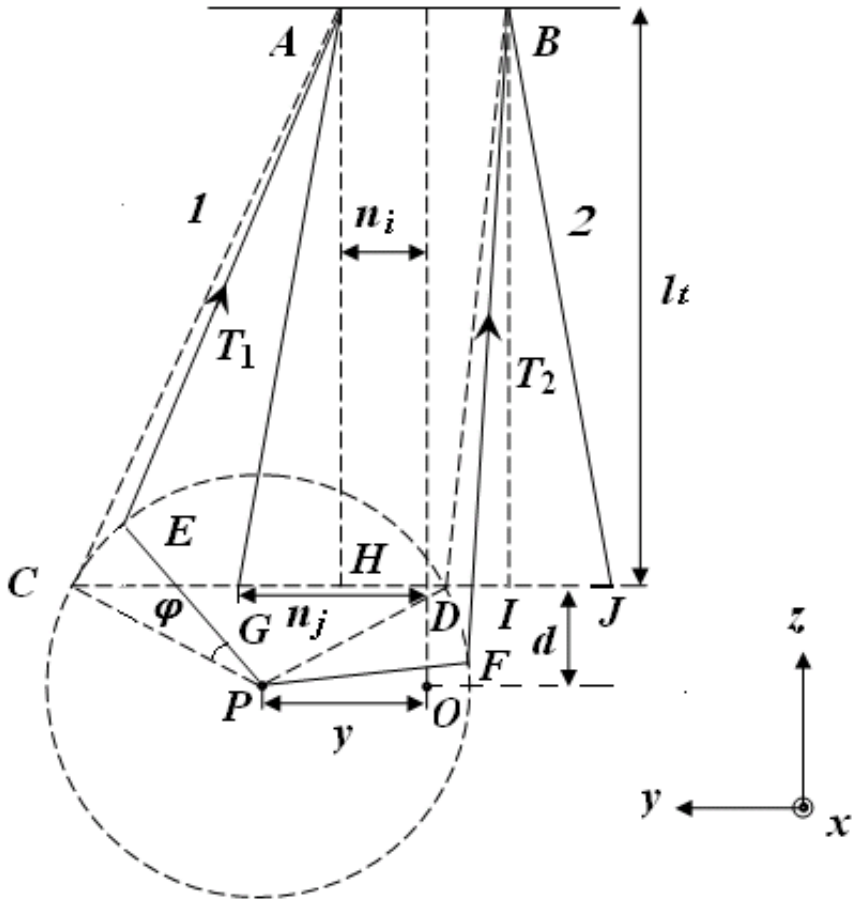

Figure 18: Face on view of the sideways and the roll motion of a single pendulum.

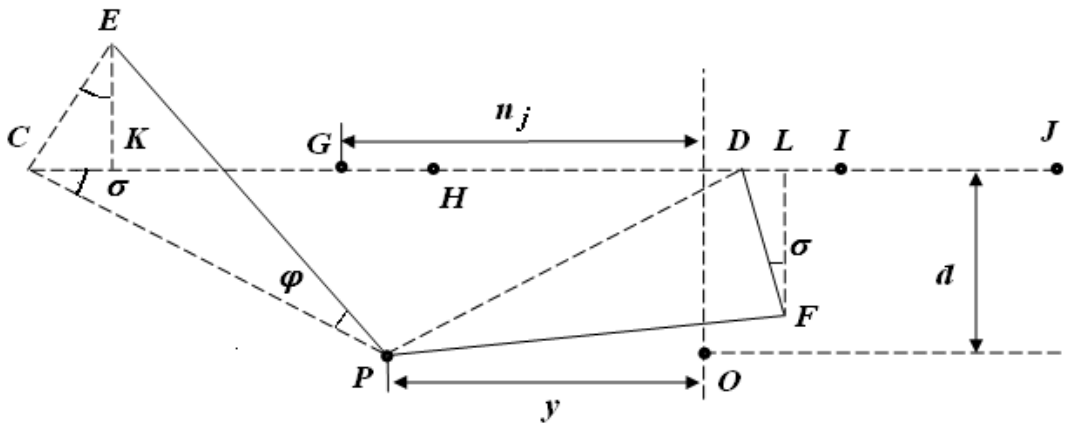

Figure 19: Expanded view of Figure 18 to show various lengths.

The sloping angle of wire 2 satisfies

$$\sin\Omega_2 = -\frac{n_j - n_i}{l} + \left[\frac{1}{l} - \frac{(n_j - n_i)^2}{l^3}\right] y - \left[\frac{d}{l} - \frac{(n_j - n_i)\,(n_j l_t + n_j d - n_i d)}{l^3}\right] \varphi, \tag{107}$$

and

$$\cos\Omega_2 = \frac{l_t}{l} + \frac{(n_j - n_i)\,l_t}{l^3} y + \left[\frac{n_j}{l} - \frac{l_t\,(n_j l_t + n_j d - n_i d)}{l^3}\right] \varphi. \tag{108}$$

The equation of motion for the displacement of the center of mass, y, is

$$m\ddot{y} = -T_1 \sin\Omega_1 - T_2 \sin\Omega_2. \tag{109}$$

Substituting for T_1, T_2 from Equation 103 and 104, for Ω_1 and Ω_2 from Equation 105, 106, 107, and 108 and using the first order approximation for small displacement y and small angle φ gives

$$\begin{aligned} m\ddot{y} = &-\left\{2k\frac{(n_j - n_i)^2}{l^2} + \frac{mg}{l_t}\left[1 - \frac{(n_j - n_i)^2}{l^2}\right]\right\} y + \\ &\left\{2k\frac{(n_j - n_i)\,(n_j l_t + n_j d - n_i d)}{l^2} + \frac{mg}{l_t}\left[d - \frac{(n_j - n_i)\,(n_j l_t + n_j d - n_i d)}{l^2}\right]\right\} \varphi. \end{aligned} \tag{110}$$

With reference to Figure 20, we can see that the component of force which rolls the mass for wire 1 is $T_1 sin\alpha$ and for wire 2 is $T_2 cos\beta$ where

$$\alpha = 90^\circ - (\sigma + \varphi) + \Omega_1, \tag{111}$$

and

$$\beta = \sigma - \varphi + \Omega_2. \tag{112}$$

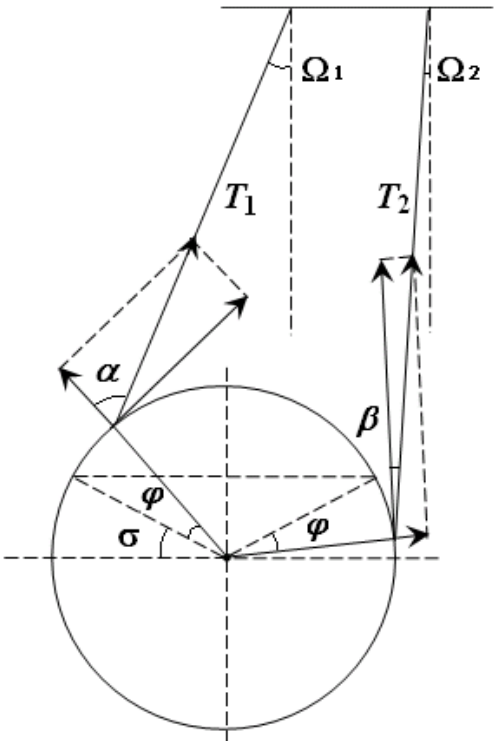

Figure 20: Tension of two wires act to roll the mass.

The angle σ is defined by the parameters of the pendulum. Using Equation 105, 106, 107 and 108, $\sin\alpha$ and $\cos\beta$ are calculated to be

$$\sin\alpha \approx \frac{n_j l_t + d\,(n_j - n_i)}{l\sqrt{n_j^2 + d^2}} + \frac{1}{\sqrt{n_j^2 + d^2}} \left\{ d \left[\frac{1}{l} - \frac{(n_j - n_i)^2}{l^3} \right] - n_j \frac{(n_j - n_i)\, l_t}{l^3} \right\} y$$
$$- \frac{1}{\sqrt{n_j^2 + d^2}} \left\{ n_j \left[\frac{n_j}{l} - \frac{l_t\,(n_j l_t + n_j d - n_i d)}{l^3} \right] + d \left[\frac{d}{l} - \frac{(n_j - n_i)\,(n_j l_t + n_j d - n_i d)}{l^3} \right] \right.$$
$$\left. - n_j \frac{n_j - n_i}{l} + d \frac{l_t}{l} \right\} \varphi, \tag{113}$$

$$\cos\beta \approx \frac{n_j l_t + d\,(n_j - n_i)}{l\sqrt{n_j^2 + d^2}} + \left\{ - \frac{d}{\sqrt{n_j^2 + d^2}} \left[\frac{1}{l} - \frac{(n_j - n_i)^2}{l^3} \right] + \frac{n_j}{\sqrt{n_j^2 + d^2}} \frac{(n_j - n_i)\, l_t}{l^3} \right\} y +$$
$$\left\{ \frac{n_j}{\sqrt{n_j^2 + d^2}} \left[\frac{n_j}{l} - \frac{l_t\,(n_j l_t + n_j d - n_i d)}{l^3} \right] + \frac{d}{\sqrt{n_j^2 + d^2}} \left[\frac{d}{l} - \frac{(n_j - n_i)\,(n_j l_t + n_j d - n_i d)}{l^3} \right] \right.$$
$$\left. + \frac{d}{\sqrt{n_j^2 + d^2}} \frac{l_t}{l} - \frac{n_j}{\sqrt{n_j^2 + d^2}} \frac{n_j - n_i}{l} \right\} \varphi, \tag{114}$$

Now the torque for the roll motion is

$$Q = \sqrt{n_j^2 + d^2}\,(T_1 \sin\alpha - T_2 \cos\beta) = \left\{ mgd \left[\frac{1}{l_t} - \frac{(n_j - n_i)^2}{l^2 l_t} \right] - mgn_j \frac{(n_j - n_i)}{l^2} + \right.$$
$$\left. 2k\, \frac{n_j l_t\,(n_j - n_i) + d\,(n_j - n_i)^2}{l^2} \right\} y - \left\{ mgn_j \left[\frac{n_j}{l_t} - \frac{(n_j l_t + n_j d - n_i d)}{l^2} \right] + mgd \left[\frac{d}{l_t} \right.\right.$$
$$\left.\left. - \frac{(n_j - n_i)\,(n_j l_t + n_j d - n_i d)}{l^2 l_t} \right] + 2k \frac{n_j l_t + d\,(n_j - n_i)}{l} \frac{n_j l_t + n_j d - n_i d}{l} + mg \left(d - \right.\right.$$
$$\left.\left. n_j \frac{n_j - n_i}{l_t} \right) \right\} \varphi. \tag{115}$$

And the equation of roll motion around the center of mass is

$$I_x \ddot{\varphi} = \left\{ mgd \left[\frac{1}{l_t} - \frac{(n_j - n_i)^2}{l^2 l_t} \right] - mgn_j \frac{(n_j - n_i)}{l^2} + 2k\, \frac{n_j l_t\,(n_j - n_i) + d\,(n_j - n_i)^2}{l^2} \right\} y -$$
$$\left\{ mgn_j \left[\frac{n_j}{l_t} - \frac{(n_j l_t + n_j d - n_i d)}{l^2} \right] + mgd \left[\frac{d}{l_t} - \frac{(n_j - n_i)\,(n_j l_t + n_j d - n_i d)}{l^2 l_t} \right] + mg \left(d - \right.\right.$$
$$\left.\left. n_j \frac{n_j - n_i}{l_t} \right) + 2k \frac{n_j l_t + d\,(n_j - n_i)}{l} \frac{n_j l_t + n_j d - n_i d}{l} \right\} \varphi. \tag{116}$$

The extension to a triple pendulum is outlined below. Although the lower mass and the intermediate mass are both suspended with four wires, the way the wires introduce the sideways and the roll motion is not different from the case where they are suspended with two wires in the manner described above. However, since what we need to consider here is the relative motion between two adjacent masses, the equations of motion become complicated. In Figure 21, the length of the suspension wires can be calculated by substituting y with $y_m - y_n$, $d\varphi$ with $d_l\varphi_m - d_u\varphi_n$, and $n_j\varphi$ with $n_j\varphi_m - n_i\varphi_n$ in Equation 99 and 102. Hence Δl becomes

$$\Delta l = \frac{n_j - n_i}{l}(y_m - y_n) - \frac{l_t}{l}(n_j\varphi_m - n_i\varphi_n) - \frac{(n_j - n_i)}{l}(d_l\varphi_m - d_u\varphi_n). \quad (117)$$

The angle of wire 1 with respect to the vertical direction Ω_1 now satisfies

$$\sin\Omega_1 \approx \frac{n_j - n_i + y_m - y_n - d_l\varphi_m + d_u\varphi_n}{l + \frac{n_j - n_i}{l}(y_m - y_n) - \frac{(n_j\varphi_m - n_i\varphi_n)\,l_t}{l} - \frac{(n_j - n_i)(d_l\varphi_m - d_u\varphi_n)}{l}} \approx \frac{n_j - n_i}{l}$$
$$\left(1 + \frac{y_m - y_n - d_l\varphi_m + d_u\varphi_n}{n_j - n_i}\right)\left[1 - \frac{n_j - n_i}{l^2}(y_m - y_n) + \frac{l_t}{l^2}(n_j\varphi_m - n_i\varphi_n) + \frac{(n_j - n_i)}{l^2}\right.$$
$$\left.(d_l\varphi_m - d_u\varphi_n)\right] = \frac{n_j - n_i}{l} + \left[\frac{1}{l} - \frac{(n_j - n_i)^2}{l^3}\right](y_m - y_n) + \frac{(n_j - n_i)\,l_t}{l^3}(n_j\varphi_m - n_i\varphi_n)$$
$$+ \left[\frac{(n_j - n_i)^2}{l^3} - \frac{1}{l}\right](d_l\varphi_m - d_u\varphi_n), \quad (118)$$

$$\cos\Omega_1 \approx \frac{l_t - n_j\varphi_m + n_i\varphi_n}{l + \frac{n_j - n_i}{l}(y_m - y_n) - \frac{(n_j\varphi_m - n_i\varphi_n)\,l_t}{l} - \frac{(n_j - n_i)(d_l\varphi_m - d_u\varphi_n)}{l}} \approx \frac{l_t}{l}$$
$$\left(1 - \frac{(n_j\varphi_m - n_i\varphi_n)}{l_t}\right)\left[1 - \frac{n_j - n_i}{l^2}(y_m - y_n) + \frac{l_t}{l^2}(n_j\varphi_m - n_i\varphi_n) + \frac{(n_j - n_i)}{l^2}(d_l\varphi_m\right.$$
$$\left.-d_u\varphi_n)\right] = \frac{l_t}{l} - \frac{(n_j - n_i)\,l_t}{l^3}(y_m - y_n) - \frac{\left(l^2 - l_t^2\right)(n_j\varphi_m - n_i\varphi_n)}{l^3} + \frac{l_t\,(n_j - n_i)}{l^3}(d_l\varphi_m$$
$$-d_u\varphi_n). \quad (119)$$

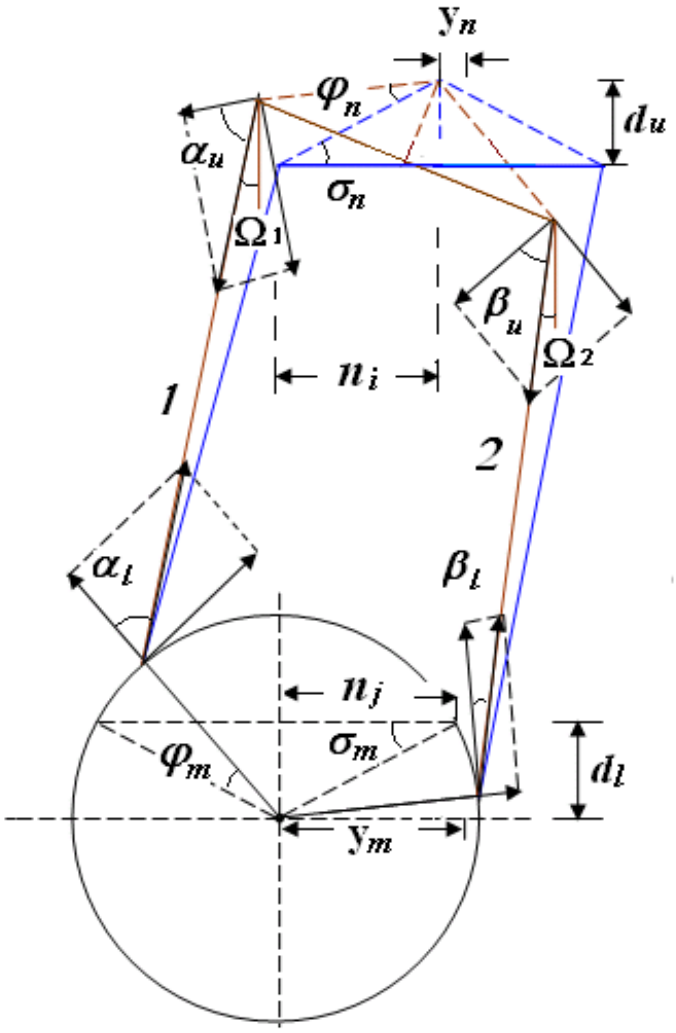

Figure 21: Sideways and roll displacements between two adjacent masses.

The sin and cos value of the sloping angle of wire 2 now become

$$\sin\Omega_2 \approx -\frac{n_j-n_i-y_m+y_n+d_l\varphi_m-d_u\varphi_n}{l-\frac{n_j-n_i}{l}(y_m-y_n)+\frac{(n_j\varphi_m-n_i\varphi_n)\,l_t}{l}+\frac{(n_j-n_i)\,(d_l\varphi_m-d_u\varphi_n)}{l}} \approx -\frac{n_j-n_i}{l}$$
$$\left(1-\frac{y_m-y_n-d_l\varphi_m+d_u\varphi_n}{n_j-n_i}\right)\left(1+\frac{n_j-n_i}{l^2}(y_m-y_n)-\frac{l_t}{l^2}(n_j\varphi_m-n_i\varphi_n)+\frac{(n_j-n_i)}{l^2}\right.$$
$$\left.(d_l\varphi_m-d_u\varphi_n)\right)=-\frac{n_j-n_i}{l}+\left[\frac{1}{l}-\frac{(n_j-n_i)^2}{l^3}\right](y_m-y_n)+\frac{(n_j-n_i)\,l_t}{l^3}(n_j\varphi_m-n_i\varphi_n)$$
$$+\left[\frac{(n_j-n_i)^2}{l^3}-\frac{1}{l}\right](d_l\varphi_m-d_u\varphi_n), \tag{120}$$

$$\cos\Omega_2 \approx \frac{l_t+n_j\varphi_m-n_i\varphi_n}{l-\frac{n_j-n_i}{l}(y_m-y_n)+\frac{(n_j\varphi_m-n_i\varphi_n)\,l_t}{l}+\frac{(n_j-n_i)\,(d_l\varphi_m-d_u\varphi_n)}{l}} \approx \frac{l_t}{l}$$
$$\left[1+\frac{(n_j\varphi_m-n_i\varphi_n)}{l_t}\right]\left[1+\frac{n_j-n_i}{l^2}(y_m-y_n)-\frac{l_t}{l^2}(n_j\varphi_m-n_i\varphi_n)-\frac{(n_j-n_i)}{l^2}(d_l\varphi_m\right.$$
$$\left.-d_u\varphi_n)\right]=\frac{l_t}{l}+\frac{(n_j-n_i)\,l_t}{l^3}(y_m-y_n)+\frac{l^2-l_t^2}{l^3}(n_j\varphi_m-n_i\varphi_n)-\frac{l_t\,(n_j-n_i)}{l^3}(d_l\varphi_m$$
$$-d_u\varphi_n). \tag{121}$$

The force on the lower mass in Figure 21 becomes

$$F=-\frac{1}{2}mg\frac{l}{l_t}(\sin\Omega_1+\sin\Omega_2)-k\Delta l\,(\sin\Omega_1-\sin\Omega_2)\approx\left\{mg\left[\frac{1}{l_t}-\frac{(n_j-n_i)^2}{l^2l_t}\right]-2k\right.$$
$$\left.\frac{(n_j-n_i)^2}{l^2}\right\}(y_m-y_n)+\left\{mg\frac{(n_j-n_i)}{l^2}+2k\frac{n_j-n_i}{l}\frac{l_t}{l}\right\}(n_j\varphi_m-n_i\varphi_n)+\left\{mg\left[\frac{(n_j-n_i)^2}{l^2l_t}\right.\right.$$
$$\left.\left.-\frac{1}{l_t}\right]+2k\frac{(n_j-n_i)^2}{l^2}\right\}(d_l\varphi_m-d_u\varphi_n). \tag{122}$$

And the equation of motion for the displacement of the lower mass m_m is

$$m_m\ddot{y}_m=R_m(y_m-y_n)+(S_mn_j-R_md_l)\,\varphi_m-(S_mn_i-R_md_u)\,\varphi_n. \tag{123}$$

Here,

$$R_m=-M_mg\left[\frac{1}{l_{tm}}-\frac{(n_j-n_i)^2}{l_m^2l_{tm}}\right]+2k_m\frac{(n_j-n_i)^2}{{l_m}^2}, \tag{124}$$

$$S_m=-M_mg\frac{(n_j-n_i)}{{l_m}^2}-2k_m\frac{n_j-n_i}{l_m}\frac{l_{tm}}{l_m}, \tag{125}$$

where M_m represents the total mass suspended on the wire. If there is no other mass suspended below m_m, $M_m=m_m$.

The angles α_l, β_l, α_u and β_u as specified in Figure 21 can be given using simple geometric analysis.

$$\alpha_l = 90^\circ - (\sigma_{mu} + \varphi_m) + \Omega_1, \tag{126}$$

$$\beta_l = \sigma_{mu} - \varphi_m + \Omega_2, \tag{127}$$

$$\alpha_u = 90^\circ - \sigma_{nl} + \varphi_n - \Omega_1, \tag{128}$$

$$\beta_u = \sigma_{nl} + \varphi_n - \Omega_2. \tag{129}$$

Therefore, the torque which rolls the lower mass is

$$\begin{aligned} Q_m^+ = \sqrt{n_j^2 + d_l^2}\left(T_1 \sin\alpha_l - T_2 \cos\beta_l\right) = \sqrt{n_j^2 + d^2}\Bigg[\frac{1}{2} M_m g \frac{l_m}{l_{tm}}\left(\sin\alpha_l - \cos\beta_l\right) + \\ k_m \Delta l (\sin\alpha_l + \cos\beta_l)\Bigg] = A_m\left(y_m - y_n\right) + B_m\left(n_j\varphi_m - n_i\varphi_n\right) + C_m\left(d_l\varphi_m - d_u\varphi_n\right) \\ + M_m g\left(n_j \frac{n_j - n_i}{l_{tm}} - d_l\right)\varphi_m, \end{aligned} \tag{130}$$

where

$$A_m = M_m g d_l \left[\frac{1}{l_{tm}} - \frac{\left(n_j - n_i\right)^2}{l_m^2 l_{tm}}\right] - M_m g n_j \frac{\left(n_j - n_i\right)}{l_m^2} + 2k_m \frac{n_j l_{tm} + d_l\left(n_j - n_i\right)}{l_m} \frac{n_j - n_i}{l_m}, \tag{131}$$

$$B_m = M_m g \frac{n_j l_{tm}}{l_m^2} - M_m g \frac{n_j}{l_{tm}} + M_m g \frac{d_l\left(n_j - n_i\right)}{l_m^2} - 2k_m \frac{l_{tm}}{l_m} \frac{n_j l_{tm} + d_l\left(n_j - n_i\right)}{l_m}, \tag{132}$$

$$C_m = M_m g \frac{n_j\left(n_j - n_i\right)}{l_m^2} + M_m g d_l \left[\frac{\left(n_j - n_i\right)^2}{l_m^2 l_{tm}} - \frac{1}{l_{tm}}\right] - 2k_m \frac{\left(n_j - n_i\right)}{l_m} \frac{n_j l_{tm} + d_l\left(n_j - n_i\right)}{l_m}. \tag{133}$$

And the torque which rolls the upper mass is

$$Q_n^- = D_n\left(y_m - y_n\right) + E_n\left(n_j\varphi_m - n_i\varphi_n\right) + G_n\left(d_l\varphi_m - d_u\varphi_n\right) + M_m g\left\{n_i \frac{n_j - n_i}{l_{tm}} - d_u\right\}\varphi_n, \tag{134}$$

where

$$D_n = M_m g d_u \left[\frac{1}{l_{tm}} - \frac{\left(n_j - n_i\right)^2}{l_m^2 l_{tm}}\right] - M_m g n_i \frac{\left(n_j - n_i\right)}{l_m^2} - 2k_m \frac{n_i l_{tm} + d_u\left(n_j - n_i\right)}{l_m} \frac{n_j - n_i}{l_m}, \tag{135}$$

$$E_n = M_m g \frac{n_i l_{tm}}{l_m^2} - M_m g \frac{n_j}{l_{tm}} + M_m g \frac{d_u\left(n_j - n_i\right)}{l_m^2} + 2k_m \frac{l_{tm}}{l_m} \frac{n_i l_{tm} + d_u\left(n_j - n_i\right)}{l_m}, \tag{136}$$

$$G_n = M_m g \frac{n_i\left(n_j - n_i\right)}{l_m^2} + M_m g d_u \left[\frac{\left(n_j - n_i\right)^2}{l_m^2 l_{tm}} - \frac{1}{l_{tm}}\right] + 2k_m \frac{\left(n_j - n_i\right)}{l_m} \frac{n_i l_{tm} + d_u\left(n_j - n_i\right)}{l_m}. \tag{137}$$

Equation 123, 130, 134 can be used as general equations to describe the roll and sideways motion of all three masses of the pendulum. The functions R, S, V A, B, C, D, E and G with variables M_m, n_i, n_j, d_l, d_u, l_m and l_{tm} need to be specified for each test mass. And $M_m = \sum_{i=m}^{3} m_i$, with $i = 1, 2, 3$.
For the lower mass,

$$m_3\ddot{y}_3 = R_3\left(y_3 - y_2\right) + \left(S_3 n_5 - R_3 d_4\right)\varphi_3 - \left(S_3 n_4 - R_3 d_3\right)\varphi_2, \tag{138}$$

$$I_{3x}\ddot{\varphi}_3 = -A_3 y_2 + A_3 y_3 - \left(B_3 n_4 + C_3 d_3\right)\varphi_2 + \left[B_3 n_5 + C_3 d_4 + m_3 g\left(n_5\frac{n_5 - n_4}{l_{t3}} - d_4\right)\right]\varphi_3, \tag{139}$$

where

$$R_3 = -m_3 g\left[\frac{1}{l_{t3}} + \frac{\left(n_5 - n_4\right)^2}{l_3^2 l_{t3}}\right] - 4k_3\left(\frac{n_5 - n_4}{l_3}\right)^2, \tag{140}$$

$$S_3 = -m_3 g\frac{\left(n_5 - n_4\right)}{l_3^2} - 4k_3\frac{\left(n_5 - n_4\right)l_{t3}}{l_3^2}, \tag{141}$$

$$A_3 = m_3 g d_4\left[\frac{1}{l_{t3}} - \frac{\left(n_5 - n_4\right)^2}{l_3^2 l_{t3}}\right] - m_3 g n_5\frac{\left(n_5 - n_4\right)}{l_3^2} + 4k_3\frac{n_5 l_{t3} + d_4\left(n_5 - n_4\right)}{l_3}\frac{n_5 - n_4}{l_3}, \tag{142}$$

$$B_3 = m_3 g\frac{n_5 l_{t3}}{l_3^2} - m_3 g\frac{n_5}{l_{t3}} + m_3 g\frac{d_4\left(n_5 - n_4\right)}{l_3^2} - 4k_3\frac{l_{t3}}{l_3}\frac{n_5 l_{t3} + d_4\left(n_5 - n_4\right)}{l_3}, \tag{143}$$

$$C_3 = m_3 g\frac{n_5\left(n_5 - n_4\right)}{l_3^2} + m_3 g d_4\left[\frac{\left(n_5 - n_4\right)^2}{l_3^2 l_{t3}} - \frac{1}{l_{t3}}\right] - 4k_3\frac{\left(n_5 - n_4\right)}{l_3}\frac{n_5 l_{t3} + d_4\left(n_5 - n_4\right)}{l_3}. \tag{144}$$

The equations for the intermediate mass are

$$\begin{aligned} &m_2\ddot{y}_2 = R_2\left(y_2 - y_1\right) + \left(S_2 n_3 - R_2 d_2\right)\varphi_2 - \left(S_2 n_2 - R_2 d_1\right)\varphi_1 - R_3\left(y_3 - y_2\right) - \\ &\left(S_3 n_5 - R_3 d_4\right)\varphi_3 + \left(S_3 n_4 - R_3 d_3\right)\varphi_2 = -R_2 y_1 + \left(R_2 + R_3\right)y_2 - R_3 y_3 - \\ &\left(S_2 n_2 - R_2 d_1\right)\varphi_1 + \left(S_2 n_3 - R_2 d_2 + S_3 n_4 - R_3 d_3\right)\varphi_2 - \left(S_3 n_5 - R_3 d_4\right)\varphi_3, \end{aligned} \tag{145}$$

$$\begin{aligned} &I_{2x}\ddot{\varphi}_2 = Q_2^+ - Q_2^- = A_2\left(y_2 - y_1\right) + B_2\left(n_3\varphi_2 - n_2\varphi_1\right) + C_2\left(d_2\varphi_2 - d_1\varphi_1\right) + \\ &\left(m_2 + m_3\right)g\left(n_3\frac{n_3 - n_2}{l_{t2}} - d_2\right)\varphi_2 - D_2\left(y_3 - y_2\right) - E_2\left(n_5\varphi_3 - n_4\varphi_2\right) - G_2\left(d_4\varphi_3\right. \\ &\left.-d_3\varphi_2\right) - m_3 g\left(n_4\frac{n_5 - n_4}{l_{t3}} - d_3\right)\varphi_2 = -A_2 y_1 + \left(A_2 + D_2\right)y_2 - D_2 y_3 - \left(n_2 B_2\right. \\ &\left.+d_1 C_2\right)\varphi_1 + \left[n_3 B_2 + d_2 C_2 + n_4 E_2 + d_3 G_2 + \left(m_2 + m_3\right)g\left(n_3\frac{n_3 - n_2}{l_{t2}} - d_2\right)\right. \\ &\left.-m_3 g\left(n_4\frac{n_5 - n_4}{l_{t3}} - d_3\right)\right]\varphi_2 - \left(n_5 E_2 + d_4 G_2\right)\varphi_3. \end{aligned} \tag{146}$$

Here

$$R_2 = (m_2 + m_3)\, g \left[\frac{1}{l_{t2}} - \frac{(n_3 - n_2)^2}{l_2^2 l_{t2}} \right] - 4k_2 \left(\frac{n_3 - n_2}{l_2} \right)^2, \tag{147}$$

$$S_2 = (m_2 + m_3)\, g \frac{(n_3 - n_2)}{l_2^2} + 4k_2 \frac{(n_3 - n_2)\, l_{t2}}{l_2^2}, \tag{148}$$

$$A_2 = (m_2 + m_3)\, g d_2 \left[\frac{1}{l_{t2}} - \frac{(n_3 - n_2)^2}{l_2^2 l_{t2}} \right] - (m_2 + m_3)\, g n_3 \frac{(n_3 - n_2)}{l_2^2} + 4k_2 \frac{n_3 l_{t2} + d_2 (n_3 - n_2)}{l_2} \frac{n_3 - n_2}{l_2}, \tag{149}$$

$$B_2 = (m_2 + m_3)\, g \frac{n_3 l_{t2}}{l_2^2} - (m_2 + m_3)\, g \frac{n_3}{l_{t2}} + (m_2 + m_3)\, g \frac{d_2 (n_3 - n_2)}{l_2^2} - 4k_2 \frac{l_{t2}}{l_2} \frac{n_3 l_{t2} + d_2 (n_3 - n_2)}{l_2}, \tag{150}$$

$$C_2 = (m_2 + m_3)\, g \frac{n_3 (n_3 - n_2)}{l_2^2} + (m_2 + m_3)\, g d_2 \left[\frac{(n_3 - n_2)^2}{l_2^2 l_{t2}} - \frac{1}{l_{t2}} \right] - 4k_2 \frac{n_3 l_{t2} + d_2 (n_3 - n_2)}{l_2} \frac{(n_3 - n_2)}{l_2}, \tag{151}$$

$$D_2 = m_3 g d_3 \left[\frac{1}{l_{t3}} - \frac{(n_5 - n_4)^2}{l_3^2 l_{t3}} \right] - m_3 g n_4 \frac{(n_5 - n_4)}{l_3^2} - 4k_3 \frac{n_4 l_{t3} + d_3 (n_5 - n_4)}{l_3} \frac{n_5 - n_4}{l_3}, \tag{152}$$

$$E_2 = m_3 g \frac{n_4 l_{t3}}{l_3^2} - m_3 g \frac{n_5}{l_{t3}} + m_3 g \frac{d_3 (n_5 - n_4)}{l_3^2} + 4k_3 \frac{l_{t3}}{l_3} \frac{n_4 l_{t3} + d_3 (n_5 - n_4)}{l_3}, \tag{153}$$

$$G_2 = m_3 g \frac{n_4 (n_5 - n_4)}{l_3^2} + m_3 g d_3 \left[\frac{(n_5 - n_4)^2}{l_3^2 l_{t3}} - \frac{1}{l_{t3}} \right] + 4k_3 \frac{(n_5 - n_4)}{l_3} \frac{n_4 l_{t3} + d_3 (n_5 - n_4)}{l_3}. \tag{154}$$

And for the top mass, the equations for the sideways and roll motion are

$$m_1 \ddot{y}_1 = R_1 y_1 + (S_1 n_1 - R_1 d_0)\, \varphi_1 - R_2 (y_2 - y_1) - (S_2 n_3 - R_2 d_2)\, \varphi_2 + (S_2 n_2 - R_2 d_1)\, \varphi_1 = (R_1 + R_2)\, y_1 - R_2 y_2 + (S_1 n_1 - R_1 d_0 + S_2 n_2 - R_2 d_1)\, \varphi_1 - (S_2 n_3 - R_2 d_2)\, \varphi_2, \tag{155}$$

$$I_{1x}\ddot{\varphi}_1 = Q_1^+ - Q_1^- = A_1 y_1 + B_1 n_1 \varphi_1 + C_1 d_0 \varphi_1 + (m_1 + m_2 + m_3)\, g \left(n_1 \frac{n_1 - n_0}{l_{t1}} \right.$$
$$\left. - d_0 \right) \varphi_1 - D_1 (y_2 - y_1) - E_1 (n_3 \varphi_2 - n_2 \varphi_1) - G_1 (d_2 \varphi_2 - d_1 \varphi_1) - (m_2 + m_3)\, g\, (n_3$$
$$\left. \frac{n_3 - n_2}{l_{t2}} - d_1 \right) \varphi_2 = (A_1 + D_1)\, y_1 - D_1 y_2 + \left[B_1 n_1 + n_2 E_1 + d_1 G_1 + (m_1 + m_2 + m_3) \right.$$
$$\left. g \left(n_1 \frac{n_1 - n_0}{l_{t1}} - d_0 \right) \right] \varphi_1 - \left[n_3 E_1 + d_2 G_1 + (m_2 + m_3)\, g \left(n_3 \frac{n_3 - n_2}{l_{t2}} - d_1 \right) \right] \varphi_2, \tag{156}$$

with

$$R_1 = -(m_1 + m_2 + m_3)\, g \left[\frac{1}{l_{t1}} - \frac{(n_1 - n_0)^2}{l_1^2 l_{t1}} \right] + 2k_1 \left(\frac{n_1 - n_0}{l_1} \right)^2, \tag{157}$$

$$S_1 = -(m_1 + m_2 + m_3)\, g \frac{(n_1 - n_0)}{l_1^2} - 2k_1 \frac{(n_1 - n_0)\, l_{t1}}{l_1^2}, \tag{158}$$

$$A_1 = (m_1 + m_2 + m_3)\, g d_0 \left[\frac{1}{l_{t1}} - \frac{(n_1 - n_0)^2}{l_1^2 l_{t1}} \right] - (m_1 + m_2 + m_3)\, g n_1 \frac{(n_1 - n_0)}{l_1^2} + 2k_1$$
$$\frac{n_1 - n_0}{l_1} \frac{n_1 l_{t1} + d_0 (n_1 - n_0)}{l_1}, \tag{159}$$

$$B_1 = (m_1 + m_2 + m_3)\, g \frac{n_1 l_{t1}}{l_1^2} - (m_1 + m_2 + m_3)\, g \frac{n_1}{l_{t1}} + (m_1 + m_2 + m_3)\, g \frac{d_0 (n_1 - n_0)}{l_1^2}$$
$$-2k_1 \frac{l_{t1}}{l_1} \frac{n_1 l_{t1} + d_0 (n_1 - n_0)}{l_1}, \tag{160}$$

$$C_1 = (m_1 + m_2 + m_3)\, g \frac{n_1 (n_1 - n_0)}{l_1^2} + (m_1 + m_2 + m_3)\, g d_0 \left[\frac{(n_1 - n_0)^2}{l_1^2 l_{t1}} - \frac{1}{l_{t1}} \right] - 2k_1$$
$$\frac{(n_1 - n_0)}{l_1} \frac{n_1 l_{t1} + d_0 (n_1 - n_0)}{l_1}, \tag{161}$$

$$D_1 = (m_2 + m_3)\, g d_1 \left[\frac{1}{l_{t2}} - \frac{(n_3 - n_2)^2}{l_2^2 l_{t2}} \right] - (m_2 + m_3)\, g n_2 \frac{(n_3 - n_2)}{l_2^2} - 4k_2 \frac{n_2 l_{t2} + d_1 (n_3 - n_2)}{l_2}$$
$$\frac{n_3 - n_2}{l_2}, \tag{162}$$

$$E_1 = (m_2 + m_3)\, g \frac{n_2 l_{t2}}{l_2^2} - (m_2 + m_3)\, g \frac{n_3}{l_{t2}} + (m_2 + m_3)\, g \frac{d_1 (n_3 - n_2)}{l_2^2} + 4k_2 \frac{l_{t2}}{l_2} \frac{n_2 l_{t2} + d_1 (n_3 - n_2)}{l_2}, \tag{163}$$

and

$$G_1 = (m_2 + m_3)\, g \frac{n_2\,(n_3 - n_2)}{l_2^2} + (m_2 + m_3)\, g d_1 \left[\frac{(n_3 - n_2)^2}{l_2^2 l_{t2}} - \frac{1}{l_{t2}} \right] + 4k_2 \frac{n_2 l_{t2} + d_1\,(n_3 - n_2)}{l_2}$$
$$\frac{(n_3 - n_2)}{l_2}. \tag{164}$$

The Equation 138, 145, 155, 139, 146, 156 are first Fourier-transformed and then rewritten in matrix form

$$\begin{pmatrix} \Lambda_{11} & \Lambda_{12} & 0 & \Lambda_{14} & \Lambda_{15} & 0 \\ \Lambda_{21} & \Lambda_{22} & \Lambda_{23} & \Lambda_{24} & \Lambda_{25} & \Lambda_{26} \\ 0 & \Lambda_{32} & \Lambda_{33} & 0 & \Lambda_{35} & \Lambda_{36} \\ \Lambda_{41} & \Lambda_{42} & 0 & \Lambda_{44} & \Lambda_{45} & 0 \\ \Lambda_{51} & \Lambda_{52} & \Lambda_{53} & \Lambda_{54} & \Lambda_{55} & \Lambda_{56} \\ 0 & \Lambda_{62} & \Lambda_{63} & 0 & \Lambda_{65} & \Lambda_{66} \end{pmatrix} \begin{pmatrix} y_1 \\ y_2 \\ y_3 \\ \varphi_1 \\ \varphi_2 \\ \varphi_3 \end{pmatrix} = \begin{pmatrix} F_s \\ 0 \\ 0 \\ Q_r \\ 0 \\ 0 \end{pmatrix}. \tag{165}$$

Here,

$$\Lambda_{11} = R_1 + R_2 + m_1\omega^2, \tag{166}$$
$$\Lambda_{12} = -R_2, \tag{167}$$
$$\Lambda_{14} = S_1 n_1 - R_1 d_0 + S_2 n_2 - R_2 d_1, \tag{168}$$
$$\Lambda_{15} = -S_2 n_3 + R_2 d_2, \tag{169}$$
$$\Lambda_{21} = -R_2, \tag{170}$$
$$\Lambda_{22} = R_2 + R_3 + m_2\omega^2, \tag{171}$$
$$\Lambda_{23} = -R_3, \tag{172}$$
$$\Lambda_{24} = -S_2 n_2 + R_2 d_1, \tag{173}$$
$$\Lambda_{25} = S_2 n_3 - R_2 d_2 + S_3 n_4 - R_3 d_3, \tag{174}$$
$$\Lambda_{26} = -S_3 n_5 + R_3 d_4, \tag{175}$$
$$\Lambda_{32} = -R_3, \tag{176}$$
$$\Lambda_{33} = R_3 + m_3\omega^2, \tag{177}$$
$$\Lambda_{35} = -S_3 n_4 + R_3 d_3, \tag{178}$$
$$\Lambda_{36} = S_3 n_5 - R_3 d_4, \tag{179}$$
$$\Lambda_{41} = A_1 + D_1, \tag{180}$$
$$\Lambda_{42} = -D_1, \tag{181}$$

$$\Lambda_{44} = B_1 n_1 + n_2 E_1 + d_1 G_1 + (m_1 + m_2 + m_3)\, g \left(n_1 \frac{n_1 - n_0}{l_{t1}} - d_0 \right) + I_{1x}\omega^2, \quad (182)$$

$$\Lambda_{45} = n_3 E_1 + d_2 G_1 + (m_2 + m_3)\, g \left(n_3 \frac{n_3 - n_2}{l_{t2}} - d_1 \right), \quad (183)$$

$$\Lambda_{51} = -A_2, \quad (184)$$

$$\Lambda_{52} = A_2 + D_2, \quad (185)$$

$$\Lambda_{53} = -D_2, \quad (186)$$

$$\Lambda_{54} = -n_2 B_2 - d_1 C_2, \quad (187)$$

$$\Lambda_{55} = n_3 B_2 + d_2 C_2 + n_4 E_2 + d_3 G_2 + (m_2 + m_3)\, g \left(n_3 \frac{n_3 - n_2}{l_{t2}} - d_2 \right) - m_3 g \left(n_4 \frac{n_5 - n_4}{l_{t3}} - d_3 \right) + I_{2x}\omega^2, \quad (188)$$

$$\Lambda_{56} = -n_5 E_2 - d_4 G_2, \quad (189)$$

$$\Lambda_{62} = -A_3, \quad (190)$$

$$\Lambda_{63} = A_3, \quad (191)$$

$$\Lambda_{65} = -B_3 n_4 - C_3 d_3, \quad (192)$$

$$\Lambda_{66} = B_3 n_5 + C_3 d_4 + m_3 g \left(n_5 \frac{n_5 - n_4}{l_{t3}} - d_4 \right) + I_{3x}\omega^2. \quad (193)$$

Hence the sideways motion induced by F_s and the roll motion induced by Q_r can be described as

$$\begin{pmatrix} y_1 \\ y_2 \\ y_3 \\ \varphi_1 \\ \varphi_2 \\ \varphi_3 \end{pmatrix} = \Xi \begin{pmatrix} F_s \\ 0 \\ 0 \\ Q_r \\ 0 \\ 0 \end{pmatrix}, \quad (194)$$

where $\Xi = \Lambda^{-1}$. The transfer functions that characterize the response of the top mass to F_s and Q_r are

$$H_{ys} = \frac{y_1}{F_s} = \Xi_{11}, \quad (195)$$

$$H_{yr} = \frac{y_1}{Q_r} = \Xi_{14}, \quad (196)$$

$$H_{\varphi s} = \frac{\varphi_1}{F_s} = \Xi_{41}, \quad (197)$$

$$H_{\varphi r} = \frac{\varphi_1}{Q_r} = \Xi_{44}. \quad (198)$$

The Bode plots for the above transfer functions are shown in Figure 22, Figure 23, Figure 24, and Figure 25 respectively.

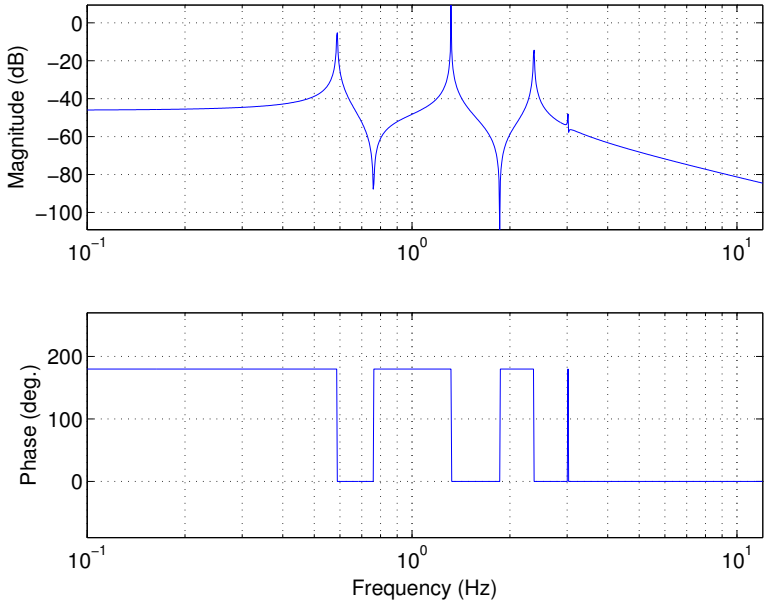

Figure 22: Bode plot of H_{ys}.

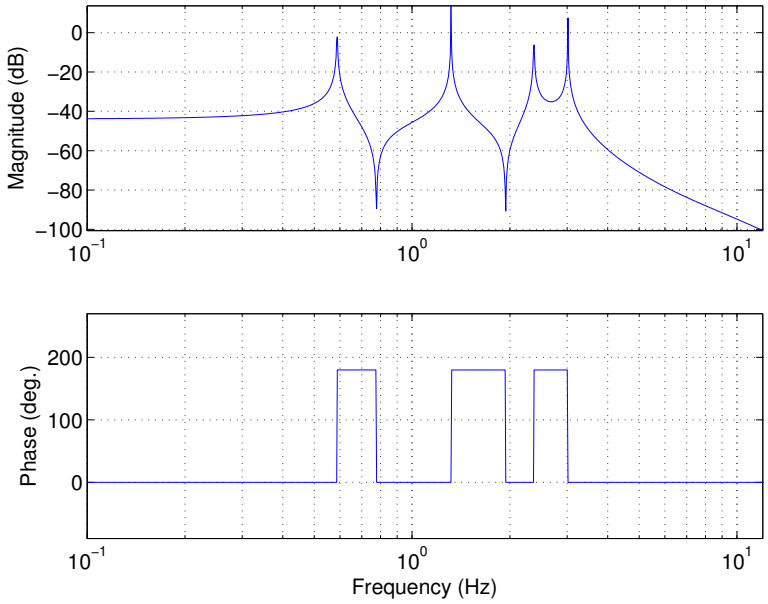

Figure 23: Bode plot of H_{yr}.

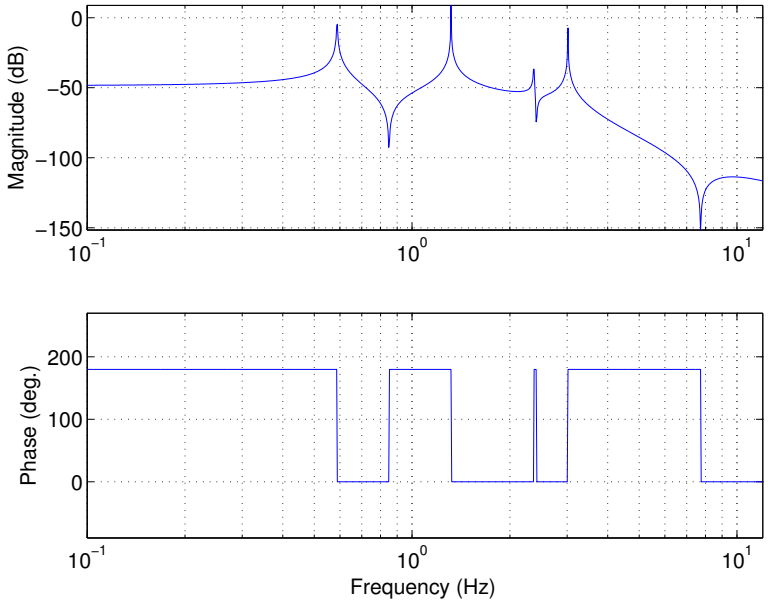

Figure 24: Bode plot of $H_{\varphi s}$.

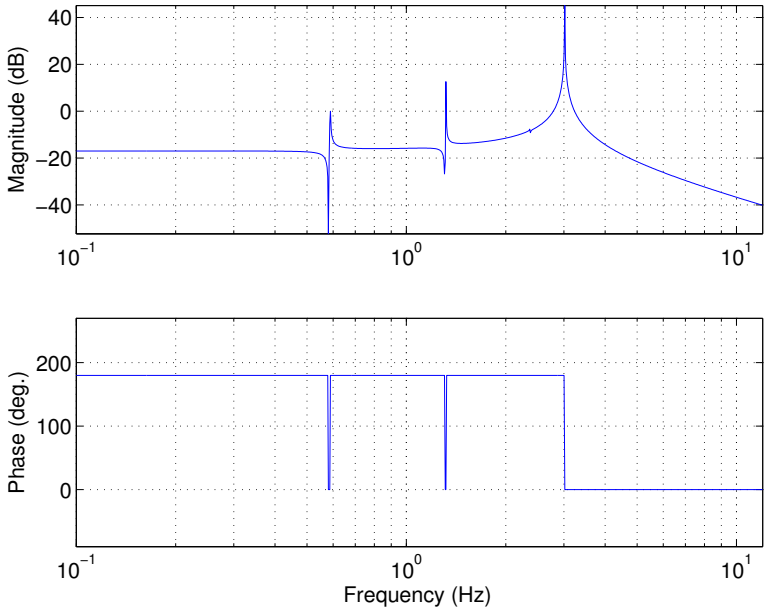

Figure 25: Bode plot of $H_{\varphi r}$.

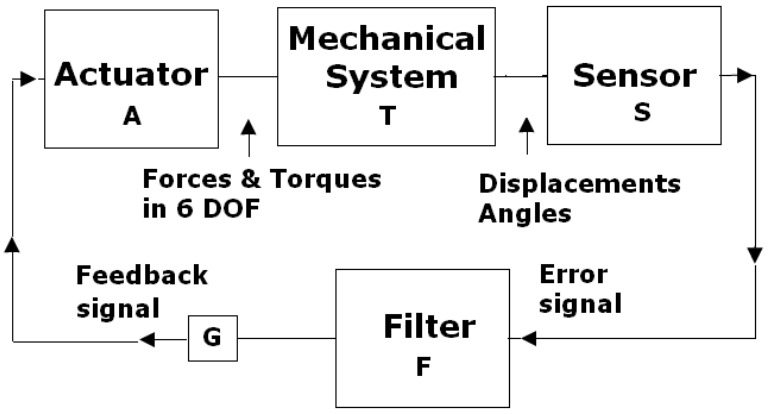

Figure 26: Feedback control block diagram of the triple pendulum. A - actuator matrix, T - system transfer function matrix, S - sensor matrix, and G - control filter.

1.4.1 Damping

Mechanical loss of the pendulum could greatly affect the sensitivity of a gravitational wave detector which use pendulums to reduce seismic noise. But it is not considered to be a big factor that will severely deteriorate the control for the suspension system at low frequencies. Although damping mechanism is complicated to be fully understood and modeled, we can simply approximate total damping effect for motions of 6 DOF by introducing viscous forces or torques which are applied on the test mass directly, using the concept of equivalent viscous damping [4]. Damping in the system is not expected to cause obvious frequency shift of the resonant modes. The viscous damping constant utilized in the model can be calibrated according to the measurement result.

1.5 Local Control of the Triple Pendulum

The resonant modes of the pendulum are damped by sensing the position of the upper mass relative to the reference pendulum or the supporting frame. Correction forces which are proportional to velocity are applied using OSEMs. Figure 1.5 shows the control loop of the triple pendulum system. The actuator, sensor and control blocks are represented by three matrices in the Matlab model. Sensor block, S, represents the calibration from position error signals to electrical current out of

the OSEM. S can be mathematically represented as

$$S=\begin{pmatrix} 1 & \mathrm{l_s} & 0 & l_\mathrm{y} & 0 & 0 \\ 1 & l_s & 0 & -l_y & 0 & 0 \\ 0 & l_p & 1 & 0 & 0 & -l_r \\ 0 & -l_p & 1 & 0 & 0 & l_r \\ 0 & 0 & 1 & 0 & 0 & -l_r \\ 0 & 0 & 0 & 0 & 1 & l_s \end{pmatrix}. \tag{199}$$

The error signal is then amplified and modified by the control loop filter to generate the feedback signal. The electrical feedback signals, variations of the current in the coil, introduce electro-magnetic force on the magnets attached on the top mass. Actuator block, A, describes the conversion from the current in the coils to the control forces and torques on the top mass. The matrix representations for S is

$$A=\begin{pmatrix} 1 & 1 & 0 & 0 & 0 & 0 \\ \mathrm{l_s} & l_s & l_p & -l_p & 0 & 0 \\ 0 & 0 & 1 & 1 & 1 & 0 \\ l_y & -l_y & 0 & 0 & 0 & 0 \\ 0 & 0 & 0 & 0 & 0 & 1 \\ 0 & 0 & l_r & l_r & -l_r & l_s \end{pmatrix}. \tag{200}$$

The transfer functions from the forces and torques to the position errors are included in block, T. The relationship between motions of the top mass and the control forces and torques can be written as

$$\begin{pmatrix} x \\ \theta \\ z \\ \phi \\ y \\ \varphi \end{pmatrix} = T \begin{pmatrix} F_l \\ Q_p \\ F_v \\ Q_y \\ F_s \\ Q_r \end{pmatrix} \tag{201}$$

And the transfer function matrix that represents T is

$$T=\begin{pmatrix} \mathrm{H_{xl}} & \mathrm{H_{xp}} & 0 & 0 & 0 & 0 \\ \mathrm{H_{\theta l}} & H_{\theta p} & 0 & 0 & 0 & 0 \\ 0 & 0 & H_{zv} & 0 & 0 & 0 \\ 0 & 0 & 0 & H_{\phi y} & 0 & 0 \\ 0 & 0 & 0 & 0 & H_{ys} & H_{yr} \\ 0 & 0 & 0 & 0 & H_{\varphi s} & H_{\varphi r} \end{pmatrix}. \tag{202}$$

The overall DC responsivity of coils, actuators and other mechanical and electrical components that build up the control loop of the suspension system is represented by block G, which consists of 6 parameters for 6 control channels, respectively. The bode plot of the control loop filter, F, is shown in Figure 1.5.

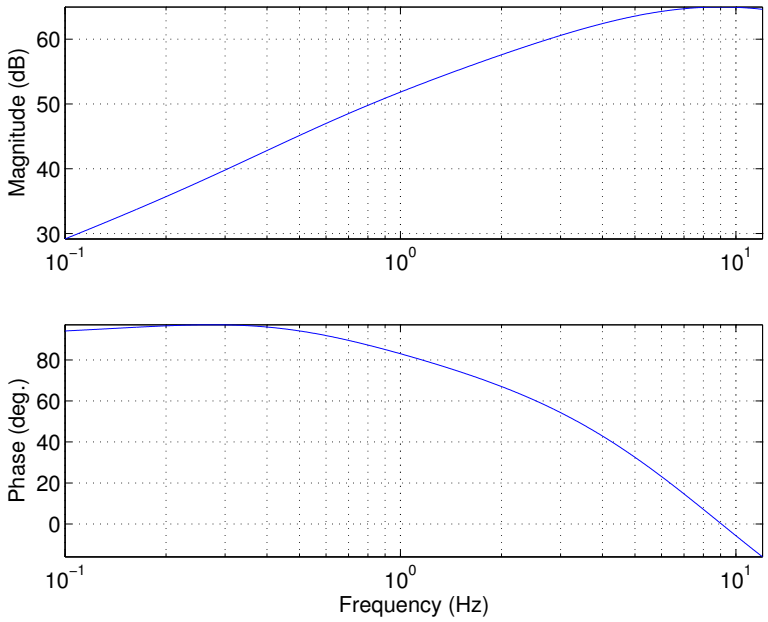

Figure 27: Bode plot for the transfer function of the control loop filter.

2 Measurement Result

To characterize the response of the pendulum to external control forces and torques, close loop transfer functions associated with various control channels were measured. These measured transfer functions can be specified by the block diagram shown in Figure 28.

The input signal, X_{in}, can be injected into single or multiple input channels to excite motions of the pendulum of different degrees of freedom while the close loop response, X_{out}, can be read from specified output channels. We can define a loop transfer function matrix, H, as

$$H = SATG. \tag{203}$$

And the closed-loop transfer function H_{cl} can be mathematically expressed as

$$H_{cl} = \frac{H_{ij}}{1 + H_{ij}H_{ji}}, \tag{204}$$

where

$$H_{ij} = \begin{cases} H(i,j) & \text{if } i \neq j \\ 1 & \text{if } i = j \end{cases}, \tag{205}$$

and

$$H_{ji} = H(j,i). \tag{206}$$

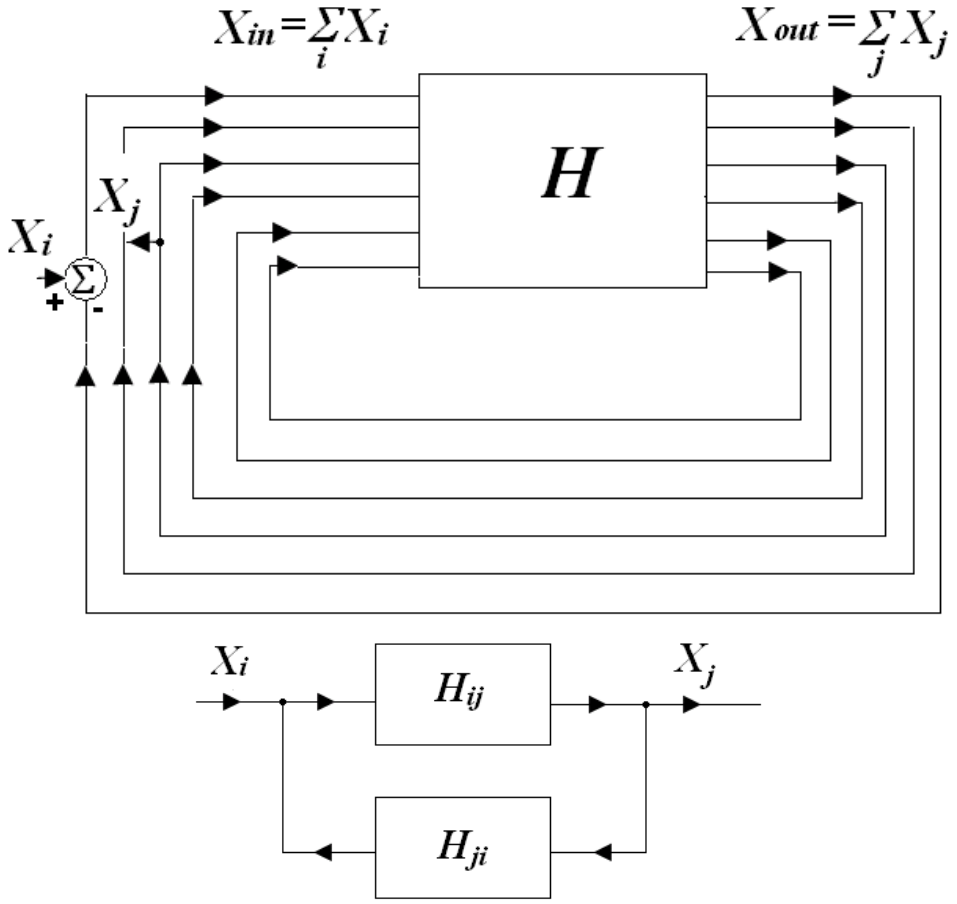

Figure 28: Block diagram used to determine the closed-loop transfer function measurement for the triple suspension system. X_{in}, X_{out} represent the input and the output signals. i and j specify the input and the output channels. H_{ij} represents the transfer functions with channel i as the input channel and channel j as the output channel (i = 1,$\cdots$ 6, j = 1,$\cdots$, 6). H_{ji} reprsents the transfer function defined vice versa.

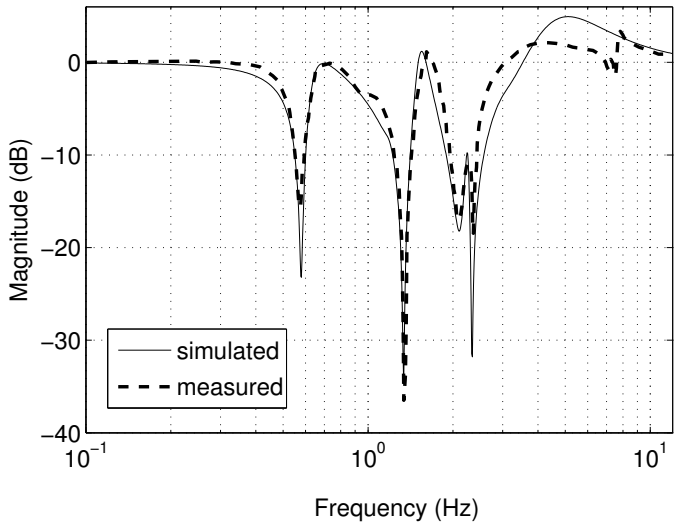

Figure 29: Measured and simulated close loop transfer functions with the input signal injected to coils 1 and 2 and the output signal read from channel 1.

Figure 29 shows the close loop transfer function with injections to channel 1 and channel 2 as the read out channel. We can clearly see the excited longitudinal mode at 6 Hz, 1.3 Hz and 2.3 Hz (Figure 11). The extra dip at around 1.9 Hz shown in the measurement result is believed to be associated with yaw motions that were excited due to the unbalanced driving on two magnets. This can be confirmed in Figure 17. The small dips located between 7 Hz and 8 Hz in the measurement curve represent motions of the supporting stack which is not considered in the matlab model. Figure 30 shows the resposne of the pendulum to an even more unbalnced driving. The 1.9 Hz Yaw mode becomes enhanced here.

Figure 31 shows a more complicated inter-channel close loop transfer function. Only one longitudinal mode at 2.4 Hz can be clearly seen here due to the strong damping effect.

We also checked the longitudianl-pitch cross coupling effect. A longitudinal force was exerted by injecting driving signals to coils 1 and 2, while pitch motions of the pendulum thus introduced was measured by reading the difference between output signals from channel 3 and channel 4. The measured result is plotted along with the simulation result in Figure 32.

Vertical motions of the pendulum can be excited by a balanced injection to coils

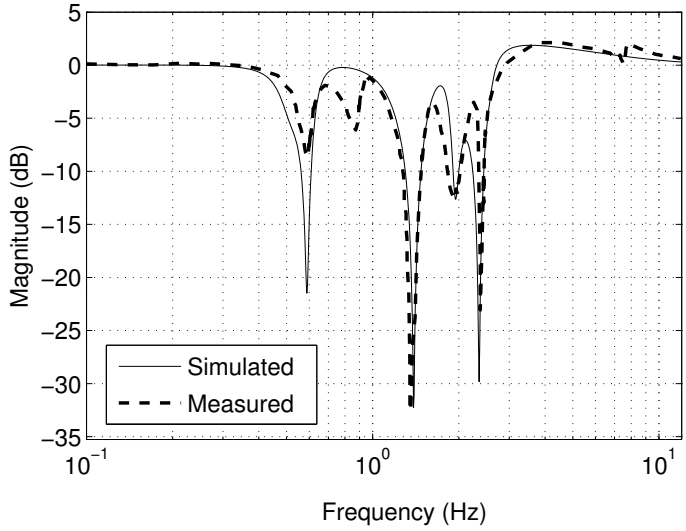

Figure 30: Measured and simulated close loop transfer functions with the input signal injected to coil 1 and the output signal read from channel 1.

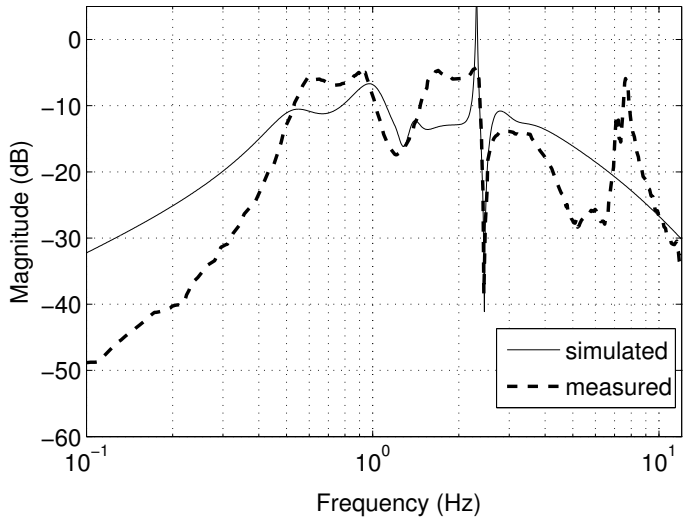

Figure 31: Measured and simulated close loop transfer functions with the input signal injected to coil 1 and the output signal read from channel 2.

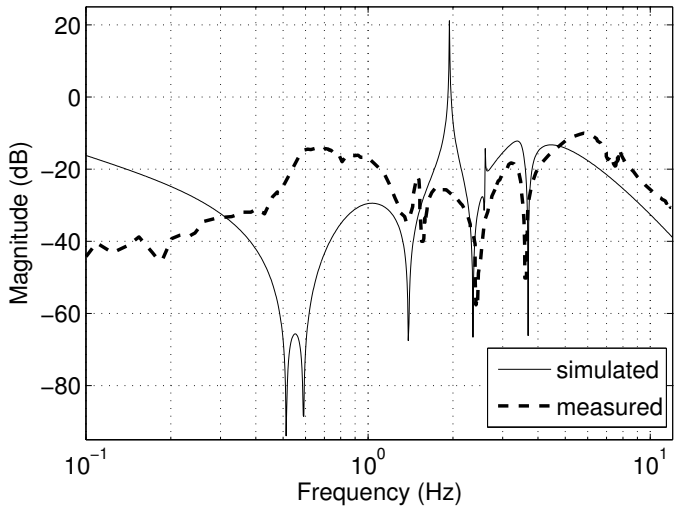

Figure 32: Measured and simulated close loop transfer functions with the input signal injected to coils 1 and 2 and the output signal read as the difference between readouts from channels 3 and 4.

3, 4 and 5. From transfer functions plotted in Figure 33 and 34, we can clearly see the excited vertical modes at 1.2 Hz and 4.8 Hz. A dual channel injection to coils 3 and 4 causes the pendulum to move vertically and roll, with sideways modtions being introduced due to the sideways/roll coupling. Figure 35 demonstrates the simulated closed loop frequency response and the measurement result for this case. Single channel injections to one of these three channels make motions of the pendulum become more complicated with pitch motions being introduced as well. The associated simulation and measurement results are plotted in Figure 36, Figure 37 and Figure 38. The curves in Figure 38 characterize the inter-channel frequency response between channel 3 and channel 4.

Sideways motions can be excited by injecting a driving signal into channel 6. The measured close-loop response is shown in Figure 39. The measured resonant modes agree well with the prediction by the matlab model.

3 Discussion

The dynamic equations derived in Section 1.1 can be easily expanded to include extra control forces and torques applied on the intermediate mass, and the lower mass as well. So the Matlab model we have built can be modified to simulate

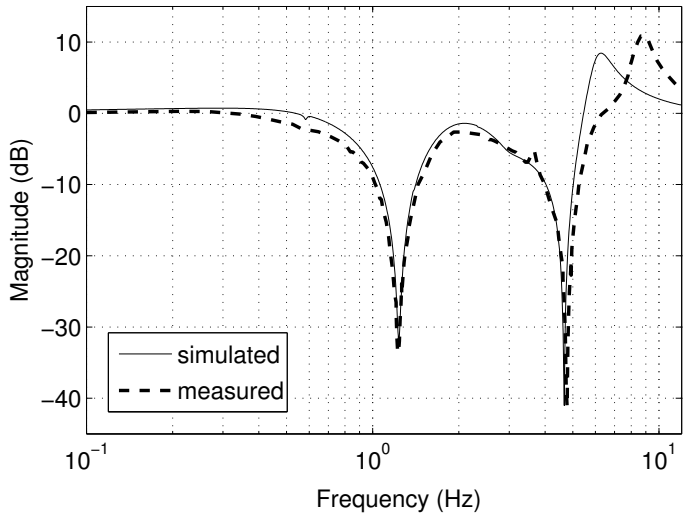

Figure 33: Measured and simulated close loop transfer function with the input signal being injected to coils 3, 4 and 5 and the output signal from channel 3.

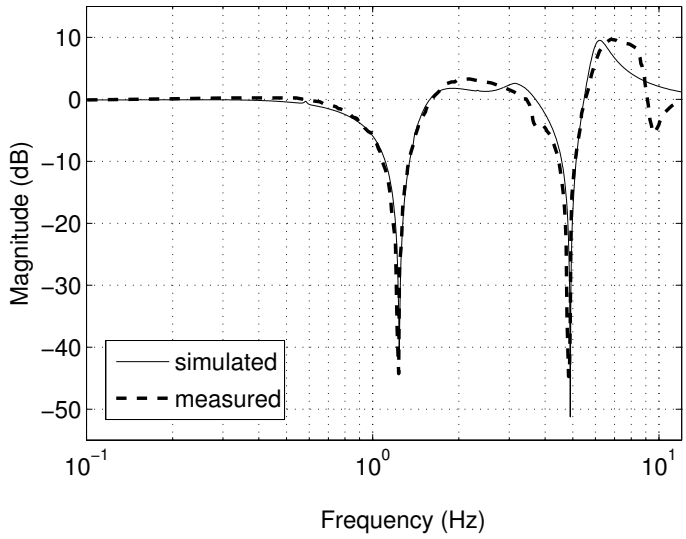

Figure 34: Measured and simulated close loop transfer function with the input signal being injected to coils 3, 4 and 5 and the output signal from channel 5.

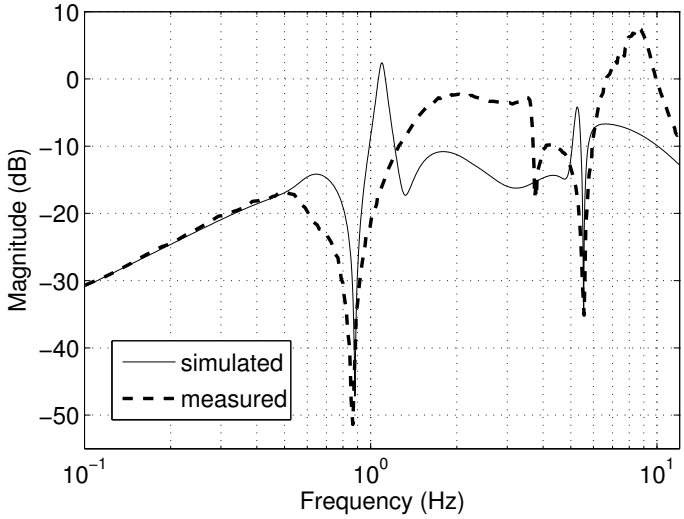

Figure 35: Measured and simulated close loop transfer functions with the input signal injected to coils 3 and 4 and the output signal read from channel 4.

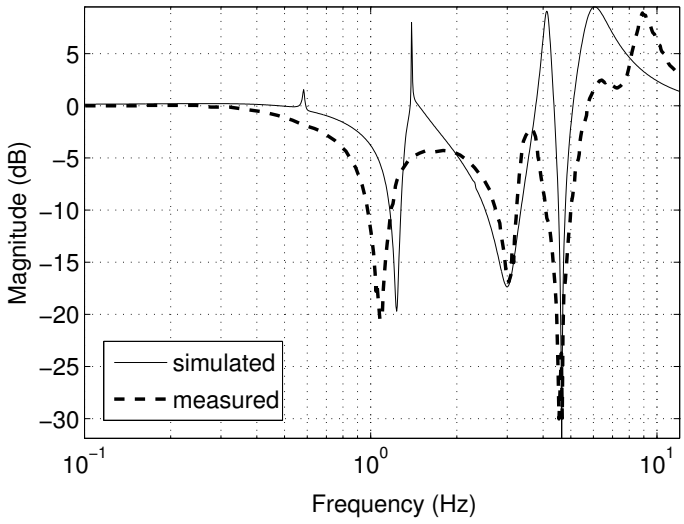

Figure 36: Measured and simulated close loop transfer functions with the input signal injected to coil 3 and the output signal read from channel 3.

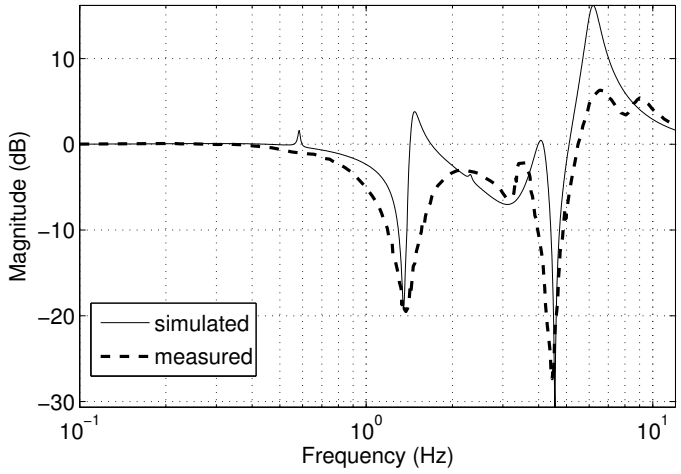

Figure 37: Measured and simulated close loop transfer functions with the input signal injected to coil 5 and the output signal read from channel 5.

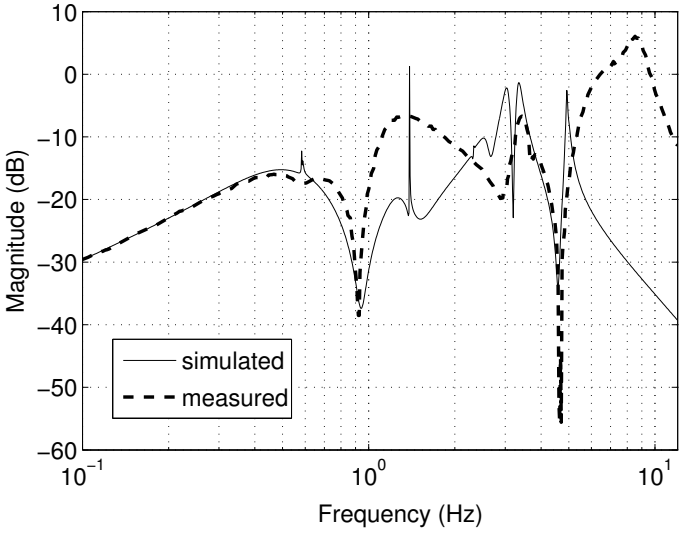

Figure 38: Measured and simulated close loop transfer functions with the input signal injected to coil 3 and the output signal read from channel 4.

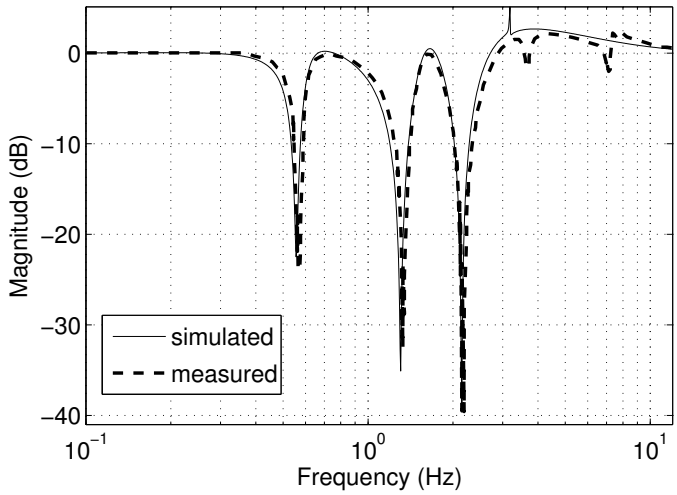

Figure 39: Measured and simulated close loop transfer function with the input signal being injected to coil 6 and the output signal from channel 6.

not only the local control scheme, but also the global control scheme. Moreover, the analysis for motions of the masses of the pendulum, which are suspended with either two wires or four wires, can generally be applied for other pendulums with similar suspension designs. Hence this model can also be viewed as an potentially useful reference model for the design of the quadruple pendulum suspension system.

References

[1] C. I. Torrie, "Development of suspension for the GEO600 gravitational wave detector," PhD thesis, Glasgow University, Glasgow, Scotland (2001).

[2] M. V. Plissi, C. I. Torrie, M. E. Husman, N. A. Robertson, K. A. Strain, and H. Ward, Rev. Sci. Instrum, **71**, 2539 (2000).

[3] W. Wan, "Instrumentation of the next generation gravitational wave detector: Triple pendulum suspension and Electro-optic modulator," PhD thesis, University of Florida, Gainesville, Flrida (1999).

[4] Paolo L. Gatti., Vittorio Ferrari *Applied Structural and Mechanical Vibrations: Theory, Methods, and Measuring Instrumentation*, (Taylor & Francis, 1999).